THE MESSENGER

EL MENSAJERO

ESO

Munich

La Silla
La Serena
Santiago

No. 23 – March 1981

Simultaneous Optical/X-ray Bursts

Jan van Paradijs, Astronomical Institute, University of Amsterdam

Introduction

The majority of the bright galactic X-ray sources are mass-exchanging binary stars in which a normal companion star is transferring matter to its compact companion, in most cases a neutron star. A neutron star is an extremely dense concentration of matter: a mass equal to that of the sun (diameter 1.4 million km) is concentrated in a sphere with a diameter of only about 20 km. The gravitational force near such a star is very strong, and, upon falling on the neutron star surface, the infalling matter reaches a velocity of about half that of light. The kinetic energy of this matter is transformed into heat (the temperature reaches values in excess of 10 million degrees) and radiated in the form of X-rays.

Almost all bright X-ray sources belong to one of the following two groups:

- Massive X-ray binaries. The companion star of the neutron star is more massive than about 10 $M_{\odot}$. These systems are young. The (rotating) neutron star has a (non-aligned) strong magnetic field, which shows up in pulsations of the X-ray emission.
- Low-mass X-ray binaries. The mass of the companion star is less than 1 $M_{\odot}$. Many of these systems emit X-ray bursts, which are the result of thermonuclear runaway processes in the freshly accreted surface layers of a neutron star.

X-ray pulsations and X-ray bursts have never been observed from the same source. This agrees with the theoretical expectation that a strong magnetic field inhibits unstable nuclear burning.

During simultaneous observations of X-ray burst sources (using X-ray satellites and optical telescopes) it was discovered that coincident with X-ray bursts a sudden increase of the optical brightness takes place.

In this article I will discuss these coincident X-ray and optical bursts, and show that such events contain information on the structure of low-mass X-ray binaries.

Observations of Optical Bursts

The first simultaneous X-ray and optical observations of X-ray bursters were made during the summer of 1977. The X-ray observations were made with the SAS-3 X-ray satellite by a group of astronomers at MIT (W. Lewin, J. Hoffman and co-workers). Optical astronomers from many countries participated in this "burstwatch", and in some cases X-ray bursts were discovered from the source 4U1837+05 (Serpens X-1) during optical coverage. (A "hit" in burster jargon). In none of these cases was there any significant increase of the optical signal during the X-ray burst, and only upper limits to the amount of energy in a possible optical burst could be given. Astronomers at the observatories of Asiago (Italy), Crimea (Soviet Union) and Kagoshima (Japan) found that less than one part in ten thousand of the X-ray burst energy was emitted in a possible optical burst.

During the summer of 1978, J. Grindlay (Harvard) and J. McClintock and C. Canizares (MIT) made a new attempt using a very sensitive photometer at the 1.5 m telescope at Cerro Tololo. The X-ray observations were again made by the MIT group using SAS-3. On June 2, 1978, the first simultaneous optical/X-ray burst was detected from the source 4U/MXB 1735–44 (see Fig. 1).

The amount of energy in the optical burst was much smaller than the upper limit found during the 1977 observations. The ratio f of the amount of energy in the optical and X-ray bursts was 2×10^{-5}. An extremely important result of this observation was that the optical

signal was delayed with respect to the X-ray burst by 2.5 to 3 seconds.

Later in the summer of 1978 an optical burst was detected from Ser X-1 by J. Hackwell, D. Gehrz, and G. Grasdalen of the University of Wyoming, using a 90 inch telescope (which was built for infrared observations). An X-ray burst was detected simultaneously with SAS-3. The ratio f turned out to be even smaller than for MXB 1735–44: only 3×10^{-6} of the X-ray burst energy turned up in the optical burst. This optical burst also was delayed, by ~ 1.5 seconds, relative to the X-ray burst.

After it was known that optical bursts do exist it was worthwhile to make a large scale observational attack, to get a better insight in their properties. Since X-ray bursts occur at intervals of hours, but sometimes do not show up for much longer periods, many nights of observing time are needed for a reasonable chance to have a "hit". During the summer of 1979 the Danish astronomer H. Pedersen of ESO spent 20 nights of observing time with the Danish 1.5 m telescope on La Silla on observations of optical bursts (*The Messenger* No. 18, 1979, p. 34).

SAS-3 hat reentered the earth's atmosphere in April 1979, but fortunately a new Japanese satellite, "Hakucho", had been launched, with which the X-ray observations were performed. The Japanese team was headed by M. Oda of the Tokyo Institute for Space Research. The X-ray and optical observations were coordinated by the SAS-3 group at MIT (L. Cominsky, G. Jernigan, W. Lewin and J. van Paradijs).

These observations were very successful: 15 optical and 16 X-ray bursts were detected from the source MXB 1636–53; in five cases a "hit" occurred.

To finish this chapter: during the summer of 1980, H. Pedersen, C. Motch and J. van Paradijs observed 25 optical bursts, four of which were detected in two or three colours simultaneously. In 6 cases there was a "hit" with Hakucho. It is still too early to give details on these most recent results.

In the following we will see how these optical burst observations can be used as probes of the structure of low-mass X-ray binary systems.

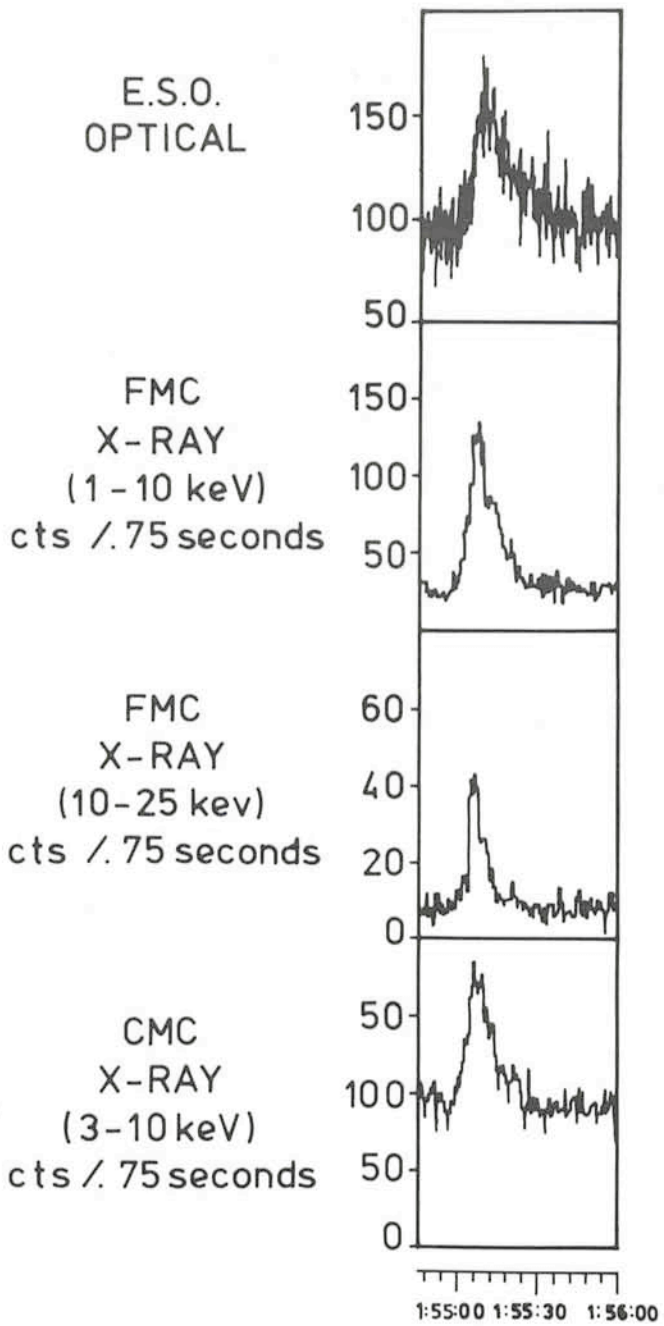

Fig. 1: *Simultaneous optical/X-ray burst observed on June 28, 1979 from MXB 1636–53. The optical burst (upper panel) was observed by Holger Pedersen with the Danish 1.5 m telescope at ESO. The X-ray burst was observed in several X-ray detectors on board the Japanese satellite Hakucho. The Hakucho team is headed by Minoru Oda. Time given is UT.*

Interpretation of Optical Burst Observations

Optical bursts contain only a very minute fraction (~ 10^{-5}) of the energy emitted in X-ray bursts. Yet this small amount is many thousand times larger than what is expected from a simple extrapolation of the observed X-ray spectrum in the burst towards the longer wavelengths in the optical passband. In combination with the observation that all observed optical bursts are delayed, this leads to the idea that they are the result of a transformation of part of the X-ray burst energy into optical radiation. The basic picture is that matter in the vicinity of the X-ray burst source absorbs a fraction of the infalling X-rays, is thereby heated, and as a consequence emits radiation at longer wavelengths.

The total pathlength for the X-rays which first travel to the absorbing matter, and of the subsequently emitted optical photons is longer than that of the X-rays which reach the observer directly. The delay of the optical signal is a natural consequence. A further contribution to the delay may be expected because the absorption of the X-rays and the reappearance of the optical photons from the absorbing medium takes a finite time. Detailed calculations show that this contribution to the delay is probably a few tenths of a second only.

Because of the finite size of the absorbing body, the optical emission from different parts of it will suffer different delays. Therefore the optical signal is not only delayed, but also smeared out. The precise values of the delay and the smearing depend on the size and shape of the region where the X-rays are reprocessed. From the observed values of delay and smearing of the optical signal one may, in turn, hope to obtain information on the location of the absorbing matter.

A method to extract this information consists of calculating synthetic optical bursts for several assumed distributions of the absorbing matter, and comparing these with the observed optical and X-ray data. In order to calculate a theoretical optical burst, a network of small surface elements is defined on the surface of the reprocessing body. Each element reflects part of the infalling X-rays and absorbs the rest. The resulting temperature of the surface element depends on the X-ray luminosity, the distance of the surface element to the X-ray source and the angle under which the X-rays reach the element. The fraction of the absorbed X-ray energy which reappears as optical photons depends on the temperature T of the surface element and on the wavelength of the photons. For high values of T most of the radiation is reemitted in the ultraviolet part of the spectrum, which cannot be observed with ground-based instruments.

By arranging the contributions of all surface elements according to their delayed arrival times we can reconstruct the profile of an optical burst as it is expected for an infinitely sharp X-ray burst. Since a real X-ray burst has a finite duration, the shape of the optical burst will be a convolution of this calculated optical response profile with the profile of the X-ray burst.

Within the framework of a low-mass X-ray binary model, obvious locations for the production of an optical burst are the surface of the companion star and an accretion disk. The latter is formed around the neutron star, because the matter which leaves the companion cannot reach the neutron star directly. Due to the rotation of the binary system, this gas flows in almost circular orbits around the neutron star. Because of mutual friction, the gas slowly spirals inward, creating a disk-shaped configuration.

The radius of the companion star is much smaller than its distance to the neutron star. Therefore the differences in the pathlength of absorbed X-rays and subsequently emitted optical photons are relatively small. Thus one expects that for optical bursts originating at the companion star, the smearing will be small compared to the average delay. For a disk, on the other hand, one expects that the smearing and delay are approximately equal. This gives us a possibility to decide where in the binary system the optical burst originates.

Detailed calculations by London, McCray and Auer (JFLA, Boulder) have shown that the optical reemission can be closely approximated by a Planckian radiation curve. For a fixed wavelength the brightness then only depends on the temperature of the radiating body. This temperature, in turn, depends on the intensity of the infalling X-rays. In this way a relation can be derived between the brightness of the X-ray source and the optical brightness of a surface element. If we wish to apply such a relation in a comparison of the observed optical and X-ray bursts, we have to realize that the temperature in the Planck function is an average over the different parts of the absorbing region.

Tentative Time-table of Council Sessions and Committee Meetings in 1981

May 4	Committee of Council
May 7 – 8	Finance Committee
May 7	Scientific Technical Committee
May 8	Users Committee
May 21 – 22	Observing Programmes Committee
June 4	Council, Stockholm
November 10	Scientific Technical Committee
November 11 – 12	Finance Committee
November 13	Committee of Council
Nov. 30 – Dec. 1 – 2	Observing Programmes Committee
December 3 – 4	Council

All meetings will take place at ESO in Garching, unless stated otherwise.

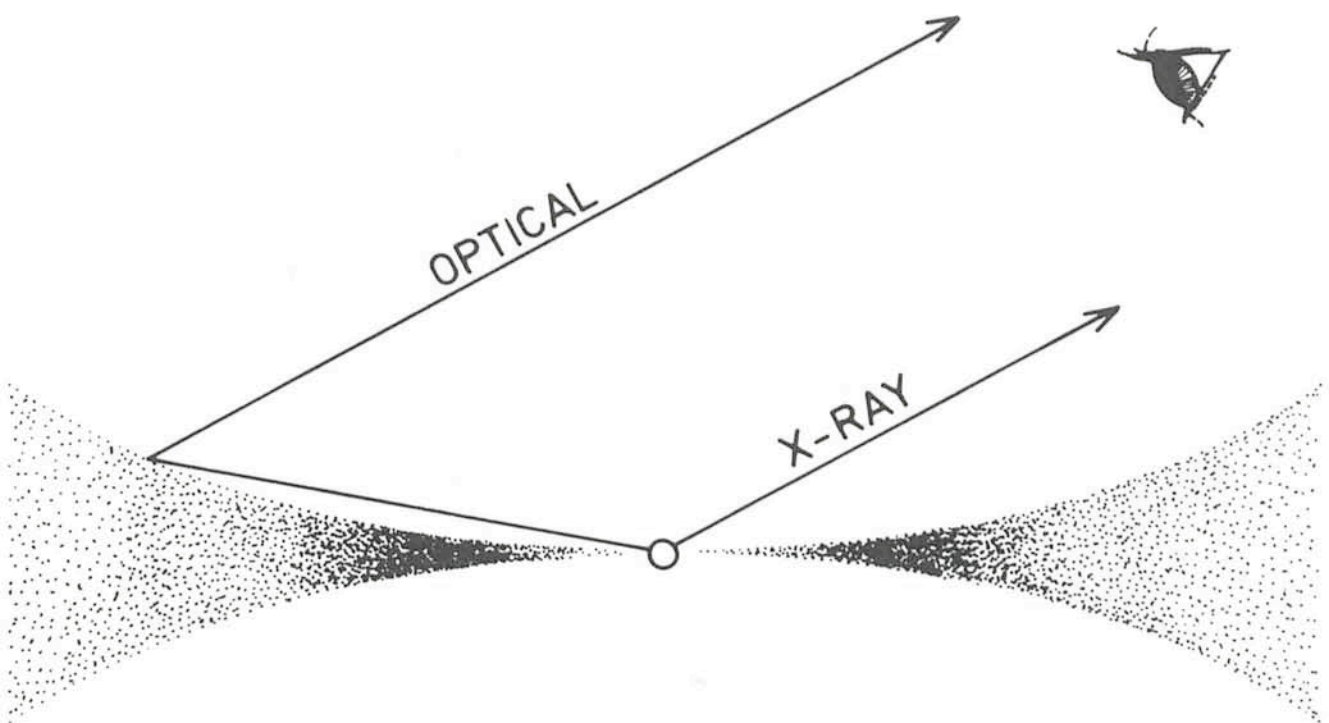

Fig. 2: *Schematic representation of the optical burst as originating from reprocessing of X-rays in an accretion disk surrounding the X-ray source.*

In an analysis procedure devised by G. Jernigan (MIT) the optical burst is considered a deformed, delayed and smeared version of the X-ray burst. The smearing is assumed to have a rectangular time dependence. The above described calculations of synthetic optical bursts indicate that this is a reasonable first approximation. The deformation is the result of the different relation of the X-ray and optical brightness to the (average) temperature of the reprocessing body.

Results

For one of the coincident optical/X-ray bursts observed in 1979 (Fig. 1), the data are of sufficient quality to determine the delay and smearing, and the temperature variation through the optical burst. For the delay and smearing, values of 3.2 ± 0.1 sec and 3.2 ± 0.4 sec were found, the maximum temperature of the reprocessing body equals 56,000 K. For two other bursts from this series, only the delay could be determined. These two optical bursts show the same delay.

These results, in particular the large value of the smearing relative to the delay, indicate that *the optical bursts originate in an accretion disk.* This is supported by the fact that all three analysed bursts yield the same value of the delay. This is expected for a circular disk: viewed from the observer such a disk always has the same location relative to the neutron star, independent of the orbital position of the companion star (Fig. 2). For optical bursts from the surface of the companion star one would expect a variable delay because of the changes in the relative positions of the observer and the binary components (unless we happen to view the binary star from a direction perpendicular to its orbital plane, or if the bursts would have occurred at the same part of the orbit).

The value of the delay is related to the size of the disk, and – indirectly – to the size of the binary system. For a given diameter of the disk the delay will be determined by the radial dependence of the contributions to the optical burst intensity (and on the angle under which the disk is seen by the observer). If the contributions from the outer parts of the disks dominate (the disk is then more nearly a ring) the delay will be maximal. The other way around, for a given delay D we may conclude that the radius of the disk is at least 0.5 D light seconds. For MXB 1636–53 this yields a minimum disk radius of 1.8 light-seconds.

The size of the disk is related to the distance between the binary components, since the disk is located inside the Roche lobe around the neutron star. This Roche lobe is a critical surface in the binary system, consisting of two separate parts, one around each of the binary components, touching each other in one single (Lagrangian) point. Particles inside this surface are unambiguously related to one of the stars, particles on or outside this surface can freely move around both stars. It is because the companion star fills its Roche lobe that matter can be transferred (through the Lagrangian point) towards the neutron star. The extent to which the accretion disk fills the Roche lobe around the neutron star is uncertain; probably its radius is between 70 and 100 per cent of that of the Roche lobe. Thus the radius of the neutron-star Roche lobe of MXB 1636–53 will be larger than 1.8 light-seconds.

The size of the Roche lobe relative to the distance between the stars depends only on the mass ratio q of the two components. For a given value R_x of the neutron-star Roche lobe the size of the Roche lobe of the comparison star is therefore a function of q only.

Mass determinations of neutron stars in massive X-ray binaries and in the binary radio pulsar show that it is reasonable to take for the neutron star mass a value of 1.4 $M_\odot$. Then for given R_x a choice of q fixes both the mass M_c of the companion and the radius R_c of its Roche lobe; stated differently, a fixed value of R_x defines a relationship between M_c and R_c.

Very probably the companion of the neutron star is a late-type main-sequence star. (In a few cases the companion of a burst source became visible after the X-rays – which dominate the optical brightness through heating – went off. In all cases the companion star turned out to be a K-type main-sequence star.) As mentioned above, in order to keep the mass transfer going, the companion has to fill its Roche lobe. Since main-sequence stars obey a well-defined mass-radius relationship, we find for a given value of R_x just one value of the companion star mass for which this is the case.

Optical burst observations only provide a lower limit to R_x, therefore we can only estimate a lower limit to M_c. For MXB 1636–53 the companion star turns out to be more massive than 0.4 $M_\odot$.

From the ratio of optical to X-ray burst energies one can, in principle, determine which fraction of the X-rays is intercepted by the disk. This would provide an estimate of the thickness of the disk, as seen from the neutron star. A problem here is that the observed optical brightness has to be corrected for the effect of interstellar extinction. If we adopt the interstellar extinction as observed for stars in the same general direction as MXB 1636–53, we find for the thickness of the disk an (uncertain) value of ~ 10 degrees.

An independent estimate of the diameter of the disk can be made from a comparison of the observed optical brightness and the surface brightness of the disk, which is determined by its (average) temperature T. (Here again we face the problem of interstellar extinction.)

Let us assume, for simplicity, that the apparent area of the disk is a circle with radius R. The optical luminosity L_{opt} of the disk is then given by

$$L_{opt} = 4\pi d^2 f_{opt} \quad \text{and also by}$$
$$L_{opt} = \pi R^2 B_{opt}(T).$$

Here d is the distance between the observer and the X-ray source, f_{opt} is the observed optical flux, and $B_{opt}(T)$ is the surface brightness of the disk (Planck function). These two expressions determine the angular diameter of the disk as seen from the earth.

There are good indications that the average maximum burst luminosity is the same for all bursts, and is approximately equal to the so-called Eddington limit. Therefore the distance to MXB 1636–53 can be estimated from the apparent maximum flux of its X-ray burst; we then get for the distance a value of ~ 5 kpc, and for the radius R of the apparent projected disk area ~ 0.5 light-seconds. This reasonably agrees with the size estimated from the delays of the optical bursts.

Applications for Observing time at La Silla

PERIOD 28

(October 1, 1981 to April 1, 1982)

Please do not forget that your proposals should reach the Section Visiting Astronomers **before April 15, 1981.**

Infrared Imaging and Speckle Observations with a TV Camera

Philippe Lamy, Laboratoire d'Astronomie Spatiale du CNRS, Marseille, and
Serge Koutchmy, Institut d'Astrophysique du CNRS, Paris

Introduction

The lack of suitable two-dimensional detectors has been a major problem for infrared imaging in astronomy, and most results so far have been obtained by scanning the object with a single detector (e. g., Terrile and Westphal, *Icarus,* **30,** 730, 1977). The relative merit of both techniques was thoroughly investigated by Hall *(Applied Optics,* **10,** 838, 1971) who concluded that, below about 2.5 μm, camera tubes should be preferred to scanners. Besides, sufficiently long times required by the scanning technique are not always available for some astronomical applications. These considerations led us to acquire a standard television camera equipped with an infrared vidicon tube N156 manufactured by Hamamatsu Co. (Japan). This tube has a PbS-PbO target whose sensitivity extends to about 2.4 μm (Fig. 1) although it has its maximum in the visible at about 0.57 μm. For such a target, theoretical considerations led to a quantum efficiency of the order of 3 x 10^{-3} at 1.6 μm and at room temperature. Our first objective was to image the thermal emission of the solar F-corona during the 1976 solar eclipse in Australia. Bad weather prevented the observation but we realized the potentiality of television imaging in the range 1-2.4 μm for other astronomical applications. This wavelength interval is interesting because it gives some access to the thermal emission of dust grains. Mapping the intensity as well as the polarization of infrared sources therefore offers a powerful means of studying their dust component. As examples, let us mention circumstellar envelopes, in particular those of carbon stars, such as IRC 10216, where considerable departure from spherical symmetry has already been observed (McCarthy et al., *Astrophysical Journal,* **235,** L27, 1980), and compact H II regions (e.g., W3). Of even greater interest is the possibility of performing speckle observations in the interval 1-2.4 μm, thanks to the short-exposure (20 msec) capability of television cameras. This technique should allow the determination of angular diameter and limb darkening of sufficiently bright stars. Two applications are worth mentioning:

(i) supergiant stars (e.g., α Ori, ο Cet, α Tau) whose diameters have already been shown to vary with wavelength (Bonneau and Labeyrie, *Astrophys. J.,* **181,** L1, 1973); Welter and Worden, *Astrophys. J.,* **242,** 673, 1980);

(ii) accreting young stars, such as the BN object and W3IRS5, which have been studied in a single radial direction by Chelli, Léna and Sibille *(Nature,* **278,** 143, 1979); as pointed out by these authors, their "specklographic" method does not allow them to answer the crucial question of the flattening in the accretion shell and its possible rotation.

We started our observations with the 1 m telescope at Pic-du-Midi Observatory *(Astronomy and Astrophysics,* **77,** 257, 1979) and showed how the smearing function improves with increasing wavelength. The "instantaneous" image structure (speckles) of α Ori was visualized in three infrared passbands as defined in Fig. 1. As expected, very few speckles were formed compared to similar experiments in the visible, since the telescope has a smaller aperture in the infrared. Furthermore, their temporal evolution was much slower than in the visible and could be followed on the monitor, although this could be due to the lag of the TV tube. Solar observations were also performed at 1.6 μm using the horizontal coelostat and included direct imagery of sunspots and simultaneous spectrography of the photosphere and sunspot umbra showing the Zeeman splitting of the Fe I line at 1.5648 μm, indicating the possibility of detecting very small-scale photospheric concentrated magnetic fields.

Stellar observations were pursued with a larger telescope, the 193 cm of Observatoire de Haute-Provence, unfortunately under poor weather conditions. Fig. 2 shows an instantaneous image of α Ori at 2 μm secured at the f/15 Cassegrain focus together with its isophote map obtained with the video-processing system of the Institut d'Astrophysique du CNRS, Paris (Coupiac and Koutchmy, *Journal of Optics,* **10,** 338, 1979). The smallest structures have a size of 0.35 arcsec, in good agreement with the resolving power of the 193 cm telescope at 2 μm.

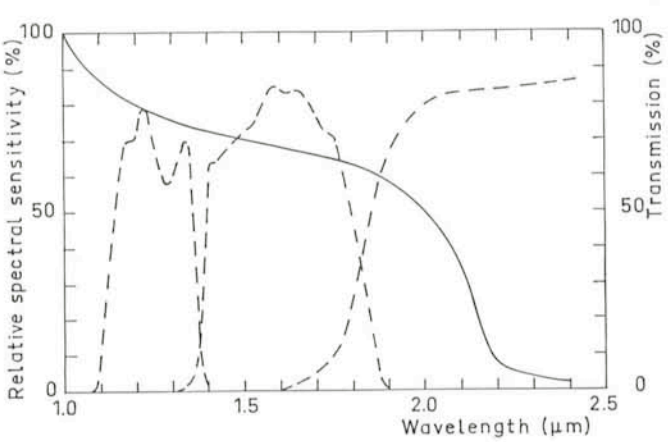

Fig. 1: *The relative spectral sensitivity of the N156 tube arbitrarily normalized at 1 μm (solid line) and the transmission curves of the filters (broken line).*

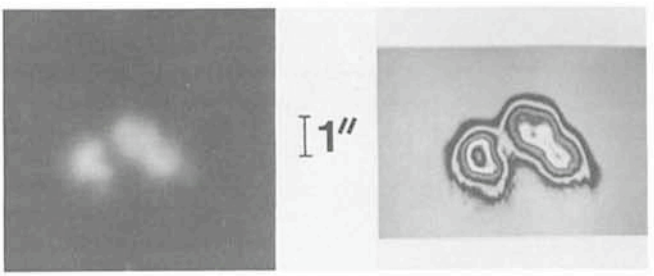

Fig. 2: *The image of α Ori at 2 μm obtained with the 193 cm telescope of Observatoire de Haute-Provence and its isophotes.*

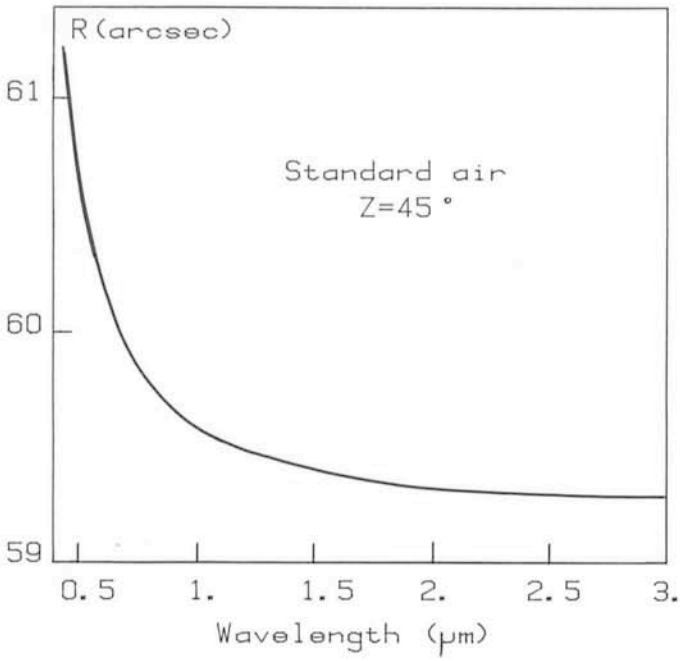

Fig. 3: *Angular deviation of light rays as a function of wavelength calculated for a standard dry atmosphere at 760 mm Hg for a zenith distance of Z = 45°.*

Note that the individual speckles are practically not lengthened by the differential atmospheric refraction, although the passband is rather large. This is because this differential effect is less severe in the infrared than in the visible. This is illustrated in Fig. 3 where we show the atmospheric dispersion as a function of wavelength (deviation angle of the light rays) calculated for a standard dry air at a pressure of 760 mm Hg and for a zenithal distance Z = 45°. This curce indicates a differential atmospheric dispersion of 3 x 10^{-2} arcsec between 1.55 and 1.8 μm. Finally, we observed more speckles than with the 1 m telescope, a sound physical result which supports the validity of our observation.

Observations at the 3.6 m Telescope

For our observations with the ESO 3.6 m telescope, we prepared a new camera completed by a video-disk and a magnetoscope. The video-disk acts as an analog memory which stores the video image which results from an integration of the target signal, a capability useful for direct imagery: in this conventional mode, the electron beam readout is cut and the target operates very much like a photographic plate. At the end of the exposure time – some 5 to 10 sec at room temperature – the readout is initiated and the video signal (one image, that is two interlaced frames) is recorded by the video-disk. Unfortunately, this video-disk was damaged during the transport and could not operate properly at the telescope, in spite of very dedicated efforts by the ESO electronic staff. Another disappointment came from the weather on La Silla which restricted our observations to episodic intervals during one night when sufficiently large holes formed in the clouds.

Direct imagery at 1.6 μm was attempted with a focal reducer working at f/1. With integration times of the order of 1 sec, Jupiter VYCMa and the η Carinae nebula were easily detected and "briefly" (for 40 msec) visualized on a TV monitor following real-time readout (no storage was possible as explained above). For the speckle observations, the focal reducer was removed and a new optical system was set up to expand the telescope focal length by a factor two (57.3 m). This moderate magnification was justified by our aim of first studying the properties of speckled images in the infrared with considerations of the signal-to-noise ratio, leaving the astrophysical aspects – which are probably even beyond the reach of a 3.6 m telescope – to a second step. Fig. 4 shows a speckled image of α Sco at 1.6 μm together with its isophote map obtained likewise that of Fig. 2. This photograph corresponds to a single frame and the size of the pixel amounts to 31 μm equivalent to 0.113 arcsec. The smallest structures have a typical size of 0.23 arcsec, in good agreement with the diameter of the Airy disk for a 3.6 m telescope at 1.6 μm. The fact that the structure of this image closely resembles that obtained at the 193 cm telescope – the number of speckles being approximately similar – remains a puzzle to us. It may be that we are reaching some limitation of the television tube. In this respect, we emphasize that all the above observations have been carried out at ambient temperature. Laboratory tests have shown that cooling the tube does have a positive effect by reducing both the lag and the thermal noise of the target; the second advantage is of particular interest for direct imagery as it allows far longer integration times. These tests are now being pursued to quantitatively assess the improved performances. We hope to come up with a better instrument and to resume our observing programme in this new and exciting field.

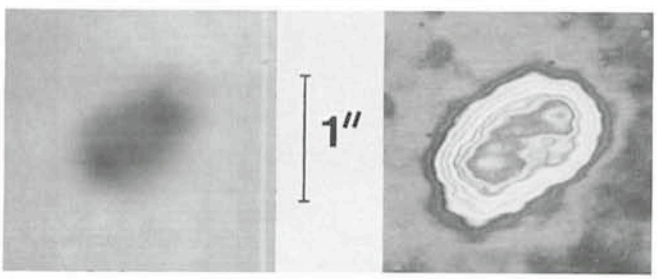

Fig. 4: *The image of α Sco at 1.6 μm obtained with the 3.6 m telescope of ESO and its isophotes. The horizontal pattern is caused by the TV raster.*

The European Space Agency (ESA) is organizing an

International Symposium on X-ray Astronomy

The symposium will take place on 22–26 June 1981 in Amsterdam. About 150 participants are expected. The deadline for applications and abstracts is 1 April 1981. The conference fee is f 150.–. For further information please contact Dr. R.D. Andresen, Space Science Department, ESTEC, Postbus 299, Noordwijk, The Netherlands.

Circumstellar Emission and Variability among Southern Supergiants

H.-A. Ott, Astronomisches Institut der Universität Münster

Introduction

Circumstellar spectral lines, especially those which directly indicate the flow of stellar material, like P Cygni lines, have been observed since the beginning of our century. The peculiar character of P Cygni itself was conspicuous on Harvard objective prism plates already in 1890. Though until today the number of these obviously mass-loosing stars grew steadily, especially since the beginning of UV astronomy, we do not know very much about the physical mechanisms which are basically responsible for the loss of stellar material. Regarding the hot stars, models are favoured in which the photospheric radiation pressure, especially in the UV, or mechanisms in stellar coronae are supposed to be the driving motors of stellar winds (see e.g. J. P. Cassinelli et al., *Publications of the Astronomical Society of the Pacific,* **90,** 496, 1978), while for the cold end of the spectral sequence, acoustic phenomena, generated in the outer stellar convection zones, seem to accelerate the outflowing masses. The medium spectral types F and G appear to show the least tendency towards mass loss. Or is it possible that the lack of suitable theories in this temperature range is at least partially responsible for the lack of systematic observations? Whether these stars are indeed more resistant to mass loss is one of the questions of our programme.

An important aspect of our programme was photometric work in addition to spectroscopic observations, because the physical processes governing the flow of stellar matter are expected to have some effect on the total electromagnetic radiation of the star. Photometric variations may reveal the regular or irregular character of these processes. Unresolved stellar companions, a possible external cause of mass loss, can be detected by light changes of the eclipsing type.

Up to now we know some stars of supergiant type Ia which have P Cygni line profiles and also show intensity variations of undeterminate character (e.g. S Doradus and the group named after it). Simultaneous spectroscopic and photometric observations of further supergiants in this programme are important in answering the questions whether this group contains particularly good candidates for stellar mass loss and what basic mechanisms play a major role in this cosmic game.

Observational Programme

We, the author in collaboration with another member of the Astronomical Institute Münster, Klaus Rindermann, observed on La Silla from July 20 to August 4, 1980. For photoelectric UBV photometry we used the 61 cm Bochum telescope during the whole period, while the coudè spectrograph at the 1.5 m ESO telescope was assigned to us for 6 parallel nights. Unfortunately the weather conditions proved to be so bad that only 5 photometric nights and 2 spectroscopic half nights, i.e. 1 effective night, remained for evaluation. The photometric quality of these nights was average to good. The scarcity of the collected data forced us, however, to eliminate some of our programme tasks from the beginning. In spite of this restriction, the observational results proved to be so interesting, that not only several of our original questions got definitive answers, but some new surprising aspects arose which deserve more observational studies. As an example we show the Hα line profiles of two G0 type stars (HR 4511 and 7066), which indicate a rather complex and certainly unusual shell structure (Fig. 1).

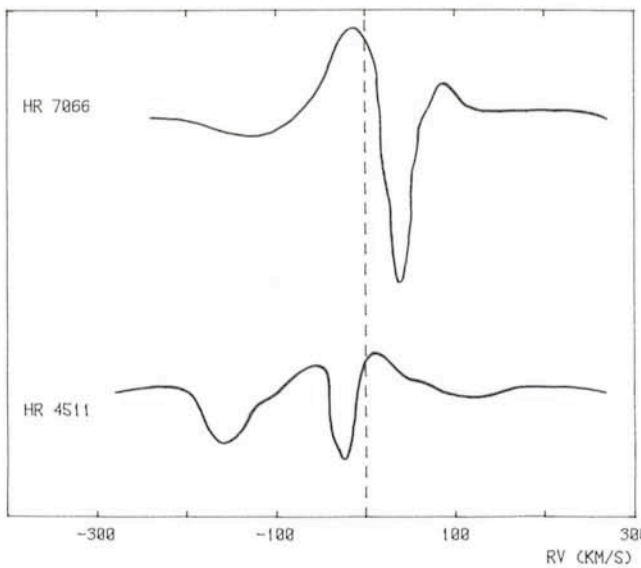

Fig. 1: *Density profiles (smoothed) of the Hα lines for two G0 type supergiant stars. The profiles are of complex P Cygni type. Given radial velocities refer to the system velocity (variable) of each star, indicated by the broken line.*

Initially our observational programme intended to answer the following questions:

1. Which and how many of the programme stars show P Cygni line profiles or at least some emission (in Hα)?
2. How large is the mass loss indicated by these lines?
3. Are there short-term (several days) spectral variations among the mass-losing stars?
4. Which and how many programme stars exhibit light and colour variations?
5. What character have these light and colour variations?
6. Are potential light variations correlated with mass loss indicators and/or spectral variations?

As programme stars we chose bright supergiants (luminosity class Ia) of spectral types B to G.

Observational Material

In order to compensate for the relatively low photometric quality of the nights, all photometric reductions of our programme stars refer to suitably chosen means of all

TABLE 1

Star (HR)	BSC: Type (LC Ia)	BSC: Var.	Spectral emission (Hα) Type	Spectral emission (Hα) RV_W (Abs.) (km/s)	Maximum deviation (V) (mag)	Maximum deviation (V) (s. d. (C))	Var.
4110	F0	V?	rev. P. Cyg	+130	0.021	2.25	V?
4147	B5				0.013	1.45	
4169	A0		P Cyg I	−168:	0.173	20.35	V
4198	B3	V?			0.029	3.42	V?
4228	A0				0.010	1.19	
4250	A0				0.008	0.91	
4337	G0		no emission				
4338	B9		rev. P Cyg	+115	0.002	0.22	
4352	F0		no emission		0.001	0.07	
4438	A0				0.056	6.05	V
4441	G0	V?			0.280	30.46	V
4442	A2				0.012	1.27	
4511	G0		P Cyg IV	−222:	0.038	4.17	V
4541	A2				0.019	2.10	V?
4644	B9				0.027	2.77	V?
4653	B2				0.017	1.87	
4876	A1	V?			0.016	2.77	V?
4887	B9				0.053	13.87	V
5379	A2		no emission		0.008	0.83	
6131	B2		P Cyg I	−198:	0.023	4.44	V
6142	B1				0.044	4.74	V
6155	B0		no emission		0.028	6.66	V
6262	B1e	V?	P Cyg I	−254:	0.021	4.16	V
6450	B4		weak emission		0.017	1.81	
6615	F2		no emission				
6812	B8p	V	P Cyg III	−98:			
6822	B0		no emission		0.014	2.89	V?
6825	A0				0.021	2.25	V?
7066	G0e	V	P Cyg IV	−225:	0.394	38.05	V

Columns 1, 2 and 3: Star number, spectral type and variability after D. Hoffleit, *Catalogue of Bright Stars* (BSC), New Haven, 1964. – Column 4: P Cygni type according to C.S. Beals, *Publ. Domin. Astrophys. Obs.*, Vol. IX, No. 1, 1950. – Column 5: Radial velocity of absorption component (wing) with respect to system velocity. – Columns 6 and 7: Maximum single deviation (absolute value) of V magnitudes from night-to-night mean differences of all comparison stars (see text), given in magnitudes (6) and in units of standard deviation of comparison stars (7). – Column 8: Variability according to our definition: V = deviation (column 7) larger than 4 standard deviations; V? = deviation between 2 and 4 standard deviations.

measurements of all comparison stars. These means are obtained from the various night-to-night differences in the V magnitudes of the comparison stars. This procedure has the additional advantage that comparison stars which are variable can easily be detected and eliminated. Most of the comparison stars are constant and, taken over the 5 good nights, show that deviations from the mean are not too large. Only two obviously variable stars (HR 6164 and 6261) have larger deviations. If we eliminate these, then the V mean difference between the first and the second night with 0.017 mag ± 0.005 (s. d.) appears to be the only significant trend. All other night-to-night differences deviate on the average by less than $0^m.01$, so that this is the upper limit for all errors due to the reduction procedure in the nights from July 21 to 30.

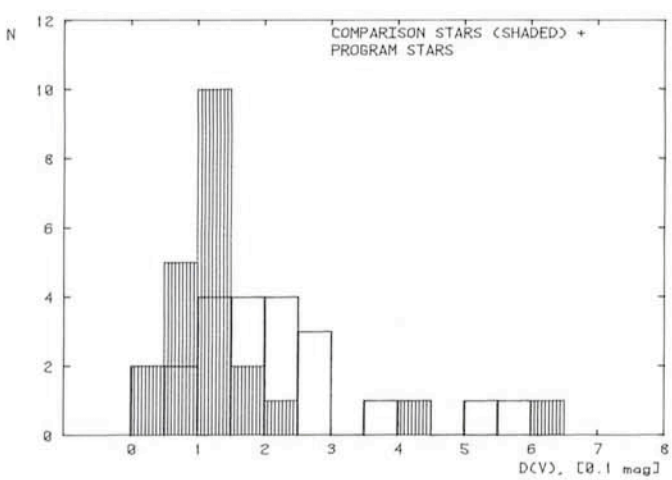

Fig. 2: *Frequency distribution of maximum single deviations (absolute value) of V magnitudes from night-to-night mean differences of all comparison stars. Two groups are plotted: all comparison stars (shaded) and all programme stars.*

A total of 26 programme stars was observed photometrically. For 15 of the programme stars we obtained coudè spectrograms on Kodak 098-04 emulsion with a dispersion of 12.4 Å/mm and a useful spectral interval between 5700 and 7300 Å.

Preliminary Results and Interpretation

Table 1 lists the preliminary results for all observed programme stars. From columns 6 and 7 we clearly see that a good number of stars have statistically significant deviations. To have a check, we computed the same

maximum single deviations for all comparison stars and compared them with those of the programme stars (Fig. 2). Here we see that the comparison stars have a distinct, small scattering frequency distribution (except for the two stars found to be variable) with a mean value near 0.012 mag – for the *maximum* deviation, *nota bene!* – the programme stars, on the other hand, show a clear displacement to larger deviations, the three extremes lying far outside of our diagram. This indicates a general tendency towards variability, especially in view of the fact that a maximum of 5 observations per star is not sufficient for catching each possible variable.

From the listed data we see:

1. 9 out of 15 stars (60%) exhibit Hα emission, 6 of them with more or less typical P Cygni line profiles (3 B, 1 A and 2 G stars, the latter with complex profiles, as shown in Fig. 1), 2 more with reverse P Cygni profiles (B, F) and 1 star with weakly indicated emission (B), possibly another P Cygni candidate.
2. The radial velocities of the P Cygni absorption components (edge of short wavelength wing) relative to the system velocities show a slight dependence on spectral type: for early B stars we find values around –200 km/s, for A stars around –100 km/s. The two G stars with complex profiles have again velocities of about –200 km/s.
3. 10 out of 26 stars (38%) are clearly variable with deviations of more than 4 standard deviations from the respective mean of the comparison stars, at least 7 more (27%) can be classified as suspected variable stars (deviations between 2 and 4 standard deviations).
4. 7 stars (78%), possibly 8 (89%), out of 9 emission line stars are variables or suspected variables. The 4 photometrically observed stars without visible emission features include 2 apparently non-variable stars (types A and G), 1 suspected (B) and 1 variable star (B).
5. Among the variables are 7 newly found variables: HR 4169, 4438, 4511, 4887, 6131, 6142, 6155.
6. Among the 17 stars of spectral types later than B9 we find the most clearly non-variable as well as the variable stars with largest amplitudes (HR 4169, 4441 and 7066), while the 9 stars of types B0 to B5 are all variable with low amplitudes (Fig. 3).

Our results may be summarized in this way:

Variability and the existence of P Cygni or emission lines in stellar spectra seem to be a rather common feature among supergiant stars of early and medium spectral types. A good correlation exists between the presence of emission lines, mainly of P Cygni type, and the presence of variability. Vice versa, this does not hold as well: variable supergiants do not always show indications of spectral emissions, at least in our limited sample of spectra. It is quite conceivable that this absence can be explained by short-term weakening of the emission lines, especially if irregular, possibly eruptive mechanisms of stellar mass loss play a role. The detection of line variations of this type was one of our original programme points which had to be omitted due to bad weather. When this weakening occurs we would generally expect a lower tendency towards variability which is not in contradiction with our data. Among the 4 non-emission-line stars we find 3 non-variables which is, compared with the emission-line stars, a distinct but not significant increase in the number of quiescent objects.

Possible quiet phases during the supergiant stage, which may be restricted to limited regions of the HRD, certainly pertain to the nature of the driving mechanisms of the mass flow. The behaviour of the early B type stars with their weak but always visible activity is sufficiently different from the behaviour of the A to G types which show a separation into inactive and strongly active groups. This is observational evidence of different driving mechanisms in addition to more theoretical considerations employed so far. For B stars the "superficial" causes (coronae, photospheric radiation pressure) may indeed be solely responsible, whereas the later stars could be transition types to the cool stars with deeper-lying phenomena related to their outer convection zones. In this intermediary group not all members may be able to fulfil the necessary conditions for being variable.

As usual we must conclude that further observations are needed. One fact however is evident: the supergiant stars, this mildly spectacular phase of stellar evolution, play a more and more important role for mass loss among stars. Possibly, they begin to rival the supernovae, these most popular objects regarding mass loss!

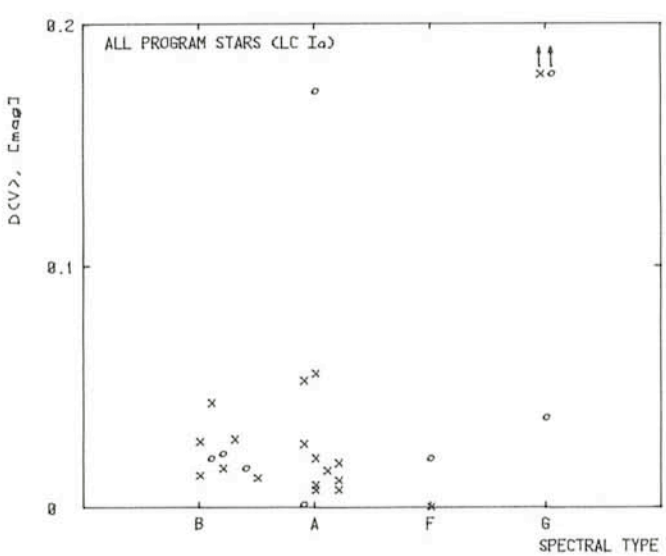

Fig. 3: *Maximum single deviation (absolute value) of V magnitudes from night-to-night mean differences of all comparison stars plotted against spectral type of each programme star. Small circles indicate stars showing Hα emission.*

Visiting Astronomers

(April 1 – October 1, 1981)

Observing time has now been allocated for period 27 (April 1 – October 1, 1981). As usual, the demand for telescope time was much greater than the time actually available.

The following list gives the names of the visiting astronomers, by telescope and in chronological order. The complete list, with dates, equipment and programme titles, is available from ESO-Garching.

3.6 m Telescope

April:	Surdej/Swings/Osmer, Schnur, Weigelt, Fitton, Fusi Pecci/Cacciari/Battistini/Buonanno/Corsi, Alcaino, Kohoutek.
May:	Kohoutek, Wehinger/Gehren/Wyckoff, Querci, F./Mauron/Perrin/Querci, M., Koornneef/Wester-

lund, Glass, Eichendorf/Glass/Moorwood, Eichendorf, Moorwood/Salinari/Shaver, Moorwood/Salinari, Motch/Ilovaisky/Chevalier, Alcaino, Valentijn, Westerlund/Richer.

June: Westerlund/Richer, Chevalier/Ilovaisky/Motch/Hurley/Niel/Vedrenne, Krautter/Reipurth, Westerlund, Wlérick/Cayatte/Bouchet, Vigroux/Comte/Lequeux/Stasinska, Gahm/Fischerström/Lindroos/Liseau, Persi/Ferrari-Toniolo/Grasdalen, Koornneef/Churchwell, Epchtein/Guibert/Nguyen Q-Rieu/Lepine/Braz, Sibille/Perrier/Léna/Foy, Bonneau/Foy.

July: Bonneau/Foy, Ardeberg/Nissen, Danks/Wamsteker, Engels, Martin/Emerson/Ruf/Wilson, Sherwood/Kreysa, Sherwood/Kreysa/Mezger, Fricke/Kollatschny/Yorke, Danziger/de Ruiter/Kunth/Lub/Griffith.

August: Danziger/de Ruiter/Kunth/Lub/Griffith, Pedersen/van Paradijs, Gyldenkerne/Axon/Taylor/Sanders/Atherton/Boksenberg, Danziger/D'Odorico/Goss/Boksenberg/Taylor, Danziger/Goss/Boksenberg/Fosbury/Axon/Taxlor, Bergeron/Boksenberg, Bergeron/Kunth/Boksenberg, Boksenberg/Danziger/Fosbury/Goss, Boksenberg/Ulrich.

September: Boksenberg/Ulrich, Lindblad/Boksenberg, Shaver, Shaver/Boksenberg, Ulrich/Boksenberg, Gillespie/Krügel/Thum, Chevalier/Ilovaisky/Motch/Hurley/Niel/Vedrenne, de Vegt, Macchetto/Perryman/di Serego Alighieri, Meisenheimer/Röser, Tarenghi/West, Wlérick/Cayatte/Bouchet, Véron, M.P. and P.

1.5 m Spectrographic Telescope

April: de Loore/Burger/van den Heuvel/van Paradijs, Richter/Huchtmeier, Richter/Materne/Huchtmeier, van Dessel, de Loore/Burger/van Dessel/van Paradijs, de Loore/Burger/van Dessel/van Paradijs, Ardeberg/Maurice, Lortet/Testor/Hydari-Malayeri, Ardeberg/Maurice.

May: Ardeberg/Maurice, Melnick/Quintana, Kohoutek, Kohoutek/Pauls, Breysacher/v. d. Hucht/Thé, Condal, Clegg/Greenberg, Krautter, Krautter/Reipurth, Piersma/Pottasch.

June: Piersma/Pottasch, Westerlund/Feinstein, de Vries/v. d. Wal, West/Kumsiachvili, Tarenghi.

July: Tarenghi, Barwig/Schoembs, Foy/Clavel/Bel, Ferlet, Ferlet/Bruston/Audouze/Laurent/Vidal-Madjar, Eichendorf, Drechsel/Rahe/Klare/Krautter/Wolf.

August: Drechsel/Rahe/Klare/Krautter/Wolf, Fricke/Kollatschny/Schleicher/Yorke, Bouchet, Ardeberg/Gustafsson, Lodén/Sundman, Pelat/Alloin, Spite, F. and M.

September: Spite, F. and M., Bouchet, Floquet/Paraggiana/Gerbaldi, Véron, P., Ferlet/Prévot, Macchetto/Perryman/di Serego Alighieri.

1 m Photometric Telescope

April: van Woerden/Danks, Alcaino, Pedersen, Wesselius/Thé, de Jong/Thé/Willems/Habing, Wlérick/Cayatte/Bouchet, Battistini/Cacciari/Fusi Pecci, Wlérick/Cayatte/Bouchet, Battistini/Cacciari/Fusi Pecci.

May: Battistini/Cacciari/Fusi Pecci, Bastien, Glass/Moorwood, Bensammar, Moorwood/Salinari, Moorwood/Salinari/Shaver, Motch/Ilovaisky/Chevalier.

June: Motch/Ilovaisky/Chevalier, Westerlund/Feinstein, Lub, Gahm/Fischerström/Lindroos/Liseau, Persi/Ferrari-T./Grasdalen, Epchtein/Guibert/Q-Rieu/Lepine/Braz, Epchtein/Gomez/Lortet, Bernard.

July: Bernard, Barwig/Schoembs, Engels, Steppe/Mezger, Bouchet, Martin/Emerson/Ruf/Wilson, Metz/Häfner.

August: Metz/Häfner, Chini, Bouchet, Heck, Gillespie/Krügel/Thum.

September: Gillespie/Krügel/Thum, Goudis/Hippelein/Münch, Hippelein/Melnick/Terlevich, Véron, M.P., Bouchet.

50 cm ESO Photometric Telescope

April: Bouchet, Lundström/Stenholm, Wesselius/Thé, Kohoutek/Knoechel, Motch.

May: Motch, Schneider/Maitzen, Schulte-Ladbeck.

June: Schulte-Ladbeck, Mauder, Bouchet.

July: Bouchet, Drechsel/Rahe/Klare/Krautter/Wolf, Metz/Häfner.

August: Metz/Häfner, Bouchet, Spite, F. and M., Lagerkvist/Rickman.

September: Lagerkvist/Rickman, Debehogne, Bouchet.

GPO 40 cm Astrograph

July: Lukas.

August: Lukas, Debehogne.

September: Debehogne.

1.5 m Danish Telescope

April: Weigelt, Veillet.

May: Motch/Ilovaisky/Chevalier, Lub.

June: Lub, Gahm/Fischerström/Lindroos/Liseau, Pedersen.

July: Pedersen, van Paradijs.

August: van Paradijs, Pedersen/van Paradijs.

September: Imbert/Prévot, Ardeberg.

50 cm Danish Telescope

September: Renson/Manfroid.

90 cm Dutch Telescope

April: Lub.

July: van Paradijs.

August: van Paradijs.

September: Isserstedt/Deubner.

61 cm Bochum Telescope

June: Bues/Rupprecht.

July: Bues/Rupprecht, Eichendorf, Schober.

August: Schober, Metz/Häfner.

September: Metz/Häfner.

The Drama of Galaxies in Close Interaction

Nils Bergvall, Astronomiska Observatoriet, Uppsala, Sweden

One of the most fundamental issues of modern astronomy is the question of the origin and early evolution of galaxies. The deeper we penetrate into the past history of the universe, the more important these questions seem to be. In particular, we may ask why the galaxies show up in so many different shapes and if the morphology of a galaxy may be substantially altered during the evolution of the universe. In this context, the galaxies which have a peculiar, i. e. non-Hubble, morphology, have attracted special attention. Among these objects, we find the interacting galaxies, which constitute approximately 5% of all galaxies.

Many interacting galaxies were once thought to be objects in rapid, violent expansion and were labelled as "post-eruptive" by Fritz Zwicky. Today, however, few people agree with this description. Instead, as has been shown by numerical modelling of close encounters between galaxies, most of these peculiar forms may be explained as effects of gravitational interaction, and we have strong reason to believe that the state of interaction may be one important stage in the evolution of many of the otherwise normal galaxies. This stage may be quite short ($\lesssim 10^9$ years) before the components of the system finally merge into one single object, thereby more or less hiding its past history. We do not know how such a merging will affect the morphology of the galaxies and neither do we know in any detail how it will affect a variety of other parameters such as star formation rate, gas/dust content and distribution, angular momentum or velocity distribution of the stars. We may assume, however, that the changes in many cases will be dramatic.

Thus, although it seems probable that many of the single galaxies that we observe today are merger remnants, our knowledge is too limited for us to be able to pick them out. It is therefore important to continue the study of galaxies in close interaction on a broad base.

Bursts of Star Formation and Nuclear Activity

In Uppsala the study of interacting galaxies in the southern hemisphere started a few years ago. Today A. Ekman, A. Lauberts and myself are working on the project. During the first years of observations, most of the data were collected at the ESO 1 m and 1.5 m telescopes and resulted in a large amount of UBV data, radial velocities and basic spectral data. A look at the radial velocity data revealed that in practically all of the observed cases the components of the systems could well be gravitationally bound. This result also implies that the galaxies normally were born side by side, although the separation between the components may have been larger in the past.

The UBV data showed that the interacting galaxies in the mean were bluer than normal, which in most cases probably is a natural consequence of the burst of star formation that is initiated by the interaction. One such unusually blue system, ESO 255-IG07, is shown in Fig. 1a. Here we see four galaxies embedded in a common halo. Although none of these galaxies is of late Hubble type, the UBV colours (U-B = –0.22, B-V = 0.54) resemble those of late-type spirals or irregulars. Spectra of these galaxies taken with the ESO 3.6 m and 1.5 m telescopes show that they contain very extended regions of ionized gas, bridging the gaps between the galaxies. These areas do not have the patchy structure characteristic of associations of H II regions, but resemble huge regions of shock-heated turbulent gas, which has been stirred up as a consequence of the interaction.

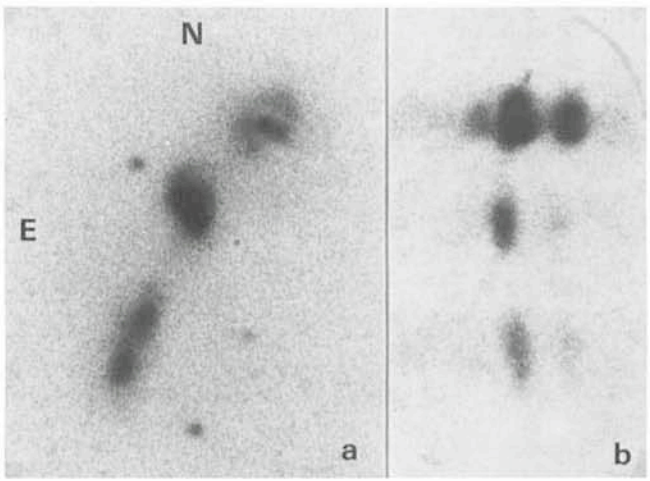

Fig. 1a: *ESO 255-IG07. 60^m prime focus plate obtained at the ESO 3.6 m telescope. Baked IIa-O emulsion + GG 385 filter.*
Fig. 1b: *The Hα region of spectra of the different components of ESO 255-IG07. The vertical scale is the same as that in Fig. 1a. Note the double structure of Hα of the northernmost component. Image tube at the Cassegrain focus of the ESO 3.6 m telescope.*

From the spectral line data, we have found evidence for shock-heating and large-scale motions of the gas clouds in the central parts of the northernmost galaxy. As can be seen from Fig. 1b, showing the spectral region around Hα, the hydrogen line is double, indicating outward flow of discrete clouds with velocities of about 150 km s^{-1}. From the [S II] λ6717/λ6731 line ratio, we know that the gas density in the central region is fairly low, about 400 cm^{-3}.

It is interesting to note that this galaxy has other features in common with galaxies with active nuclei. The form of the Balmer decrement and the strong Na I D lines in absorption imply that it contains huge amounts of dust, causing an absorption of about 4^m in blue. If this envelope would disperse, we would see a brilliant small nucleus of an unusually high surface brightness. A detailed analysis of the properties of this system will soon appear in *Astronomy and Astrophysics.*

First Act: A Close Encounter in Slow Tempo

Naturally, it would be interesting to know more about the features of the nuclei of interacting galaxies in relation to the often very chaotic state of the interstellar medium, in the cases where the components have interpenetrated

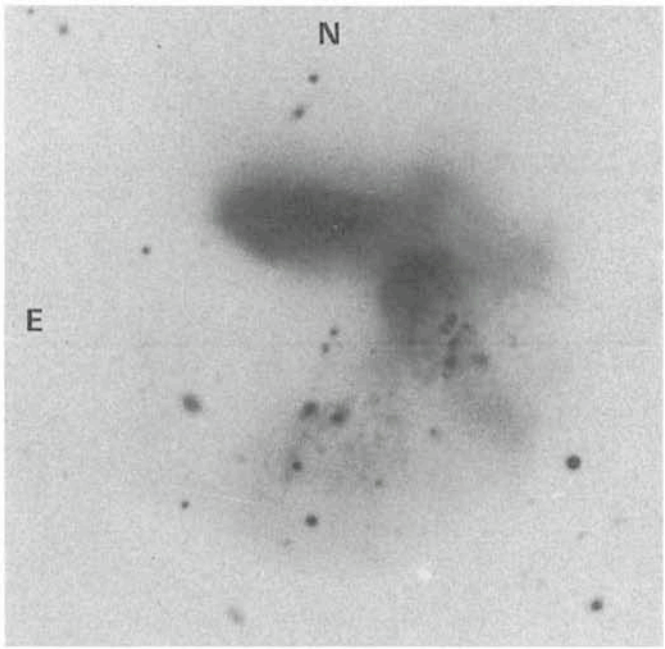

Fig. 2: *NGC 454. 90^m prime focus plate at the ESO 3.6 m telescope. Baked IIIa-J + GG 385 filter.*

deeply. At the moment, therefore, we have devoted much of our attention to the study of such systems, one of which is shown in Fig. 2. This blue photograph of NGC 454 was obtained at the prime focus of the ESO 3.6 m telescope. Here we witness how two galaxies, one of early and one of late Hubble type, have advanced into the merging state. As can be seen from the deep blue photo, although mostly exceedingly faint, the system is limited by a remarkably regular envelope.

Fig. 3 shows spectra of the central regions of the two components of NGC 454, obtained with the Image Dissector Scanner at the ESO 3.6 m telescope. The westernmost galaxy shows a spectrum typical of H II regions and has a very blue continuum. This probably originates from hot stars, rapidly being formed in the vicinity of the nucleus. The eastermost component also shows the nebular [O III] lines in emission, but no Hβ in emission – a remarkable circumstance. Either it means that the excitation is high, which is contradicted by the absence of high ionization lines, like He II λ4686, or the underlying stellar absorption is strong. We favour the last interpretation, since the Balmer lines in absorption are clearly seen at the blue end.

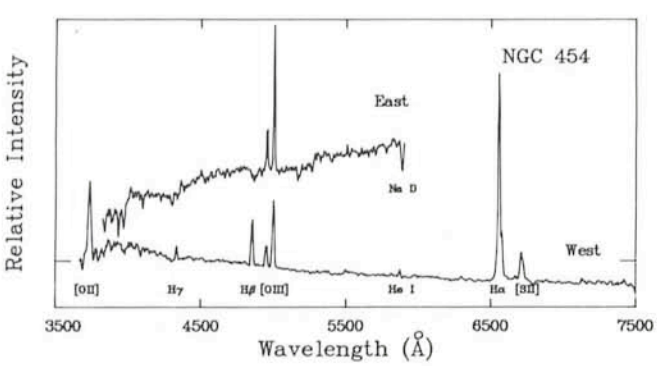

Fig. 3: *Spectra of the two nuclei of NGC 454, obtained with the IDS at the ESO 3.6 m telescope.*

Thus, young stars may give an important contribution to the light of the blue region also in this case. The red colour of the continuum is probably due to reddening by dust in the central region. The strong Na I D and probably also Ca II H and K are thus largely interstellar in origin.

According to the UBV data, NGC 454 east mainly contains old stars. Most of the star formation activity is thus confined to the nucleus. From where then does the fuel of this star formation come? It seems likely that it is supplied by the gas-rich companion galaxy, or that unprocessed halo gas, through the effects of the interaction, is accreted onto the nucleus, thereby initiating the star formation.

Final Act: The Two Become One

Systems like NGC 454 make it tempting to speculate about what a completely merged system of this type could look like. It seems that it should have a fairly regular shape and an early stellar population dominating the light of the nucleus, if the merging took place recently. The gas content should have gone down considerably, due to the high rate of star formation. Still, it could be normal, in relation to the morphological type, if the process of merging has caused a drift towards earlier Hubble types, as expected.

About 20% of all disturbed galaxies appear as single, isolated galaxies. A few of these may be the objects we are looking for, and Fig. 4 shows one possible candidate, ESO 341-IG04, although one may think of alternative interpretations of the peculiar properties of this system. The total dimension is about 50 kpc and $M_V = -21.9$ ($H_O = 75$ km^{-1} Mpc^{-1}), which is unusually bright. Morphologically, we notice the structures of the outer regions, which may be remnants of spiral arms from a galaxy that has participated in the merging.

In Fig. 5 we see the spectrum of the central region. Despite the early morphological type, which suggests that the light should be dominated by that of old stars, the spectrum comes from a fairly young stellar population, showing strong Balmer lines in absorption. At Hα, emission is also seen. A long-exposed spectrum obtained at the 1.5 m telescope shows that the young population dominates the light out to about 3 kpc from the centre. The corrected UBV colours (U-B = 0.36, B-V = 0.70) are practically independent of aperture and deviate strongly from the two-colour relation of normal galaxies. The colours are not abnormal, however, compared to colours from models of galaxies invoking an intense burst of star formation in an old stellar population (Larson and Tinsley: 1978, *Astrophysical Journal* **219,** 45). The best agreement is found if the maximum of the burst occurred about $2 \cdot 10^9$ years ago, in agreement with the timescale of the merging and the composite spectral type.

Near-infrared Photometry

As an additional source of information about the conditions in the central regions of interacting galaxies, we have used broadband near-infrared photometry. Using the InSb detector at the ESO 1 m telescope we have obtained JHKL magnitudes at 12″ aperture. Fig. 6 shows the results combined with the UBV data, for NGC 454 and ESO 341-IG04. Normally, the IR continuum of galaxies, being

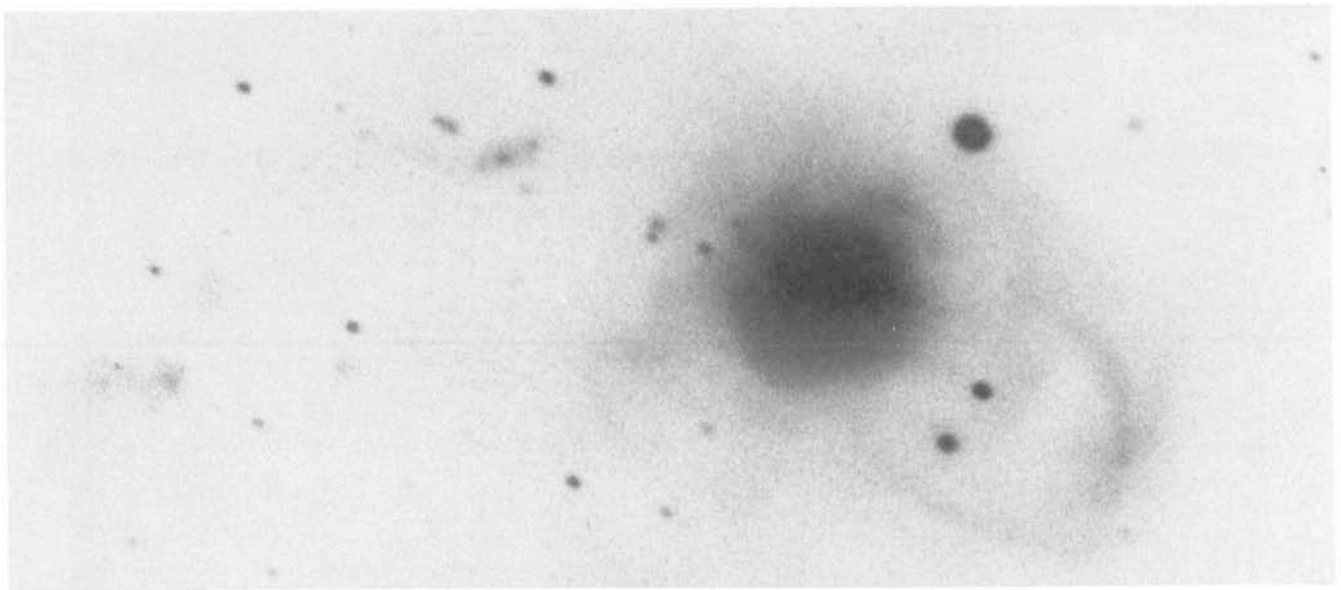

Fig. 4: *ESO 341-IG04. 75^{m} prime focus plate at the ESO 3.6 m telescope. Baked IIIa-J + GG 385 filter.*

dominated by late-type giants, reaches a maximum around H. NGC 454 east, however, keeps on rising towards lower frequencies after a local maximum. This part of the continuum probably originates from dust that has been heated by hot stars in the nuclear region, in agreement with the description given above. ESO 341-IG04, although having a K excess as compared to normal galaxies, seems to possess considerably less dust in front of the hot stars, or the heating of the dust is less efficient. The fact that Na I D is strong seems to favour the last alternative, but the analysis is still very preliminary.

Another important aspect of IR observations of interacting galaxies is the possible link to Seyfert 2 galaxies, which also show spectra that rise steeply into the infrared. The mechanism behind this radiation is still in many cases unclear.

Present Status and Future Observations

During the last few years we have obtained a large amount of detailed spectroscopic, photographic and photometric data of interacting galaxies. Most of these objects are cases where galaxies of fairly ordinary dimensions and luminosities are involved, as in the cases discussed above. Another subgroup is characterized by aggregates of small (young?) irregular blue objects, which seem to be underabundant of heavy elements. The analysis of all these data is now in full progress. An exciting future project would be to use the results of the analysis in a search for "merger remnants" among galaxies resembling ordinary E – S0's. This would not have much connection with the models of cluster cannibalism, since these so far only involve regular gas-free galaxies. As concerns the fate of merging spiral galaxies, it seems that the breakthrough in the understanding of these objects must be preceded by extensive observations over the whole accessible wavelength region.

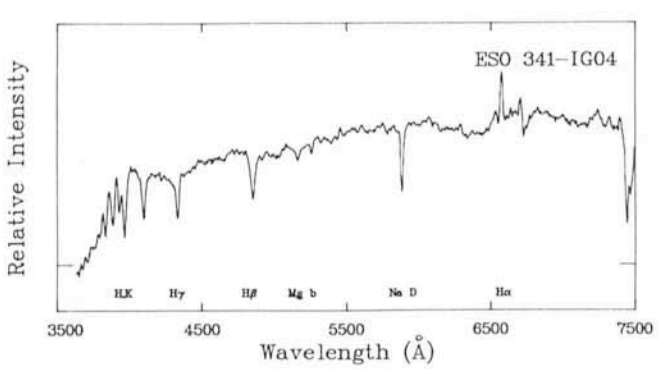

Fig. 5: *Spectrum of centre of ESO 341-IG04, obtained with the IDS at the ESO 3.6 m telescope.*

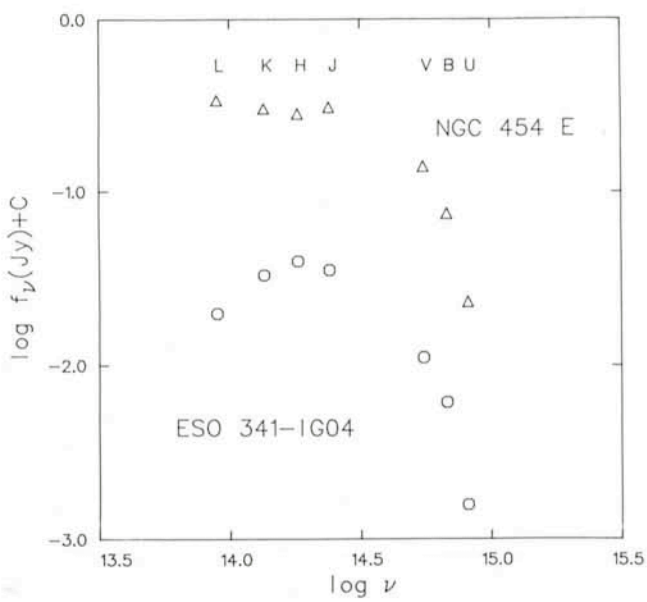

Fig. 6: *Photoelectrical broadband photometry of NGC 454; aperture: 12" (JHKL) and 22" (UBV), and ESO 341-IG04; aperture: 12" (JHKL) and 11" (UBV). C = 1 for NGC 454 and C = 0 for ESO 341-IG04.*

ANNOUNCEMENT OF AN ESO CONFERENCE

Scientific Importance of High Angular Resolution at Infrared and Optical Wavelengths

The European Southern Observatory is organizing an international conference on the subject "SCIENTIFIC IMPORTANCE OF HIGH ANGULAR RESOLUTION AT INFRARED AND OPTICAL WAVELENGTHS", to be held in the ESO building at Garching bei München during the period of 24–27 March 1981.

The purpose of this conference is to discuss, on the one hand, the systems in use or under construction and possible future developments to achieve high angular resolution and, on the other hand, to discuss the areas of astrophysics which, in the next decades, will most benefit from observations at high angular resolution.

PROGRAMME

I. Light Propagation in the Atmosphere and Image Formation

F. Roddier (Nice)	Atmospheric Limitations to High Angular Resolution Imaging
J.W. Hardy (ITEK Corp.)	Active Optics in Astronomy

II. Speckle Interferometry

A. Labeyrie (CERGA)	Review of the Field and Trends
G. Weigelt (Erlangen)	Speckle Interferometry and Speckle Holography
P. Léna (Meudon)	Speckle Interferometry in the Infrared
J.E. Nelson (Berkeley)	Coherent Large Telescopes

III. Interferometry with Multiple Systems

C.H. Townes (Berkeley)	Multiple Telescope Interferometry in the Infrared
A. Labeyrie (CERGA)	Multiple Telescope Interferometry: Compact or Diluted Telescopes?
F.J. Low (Tucson)	Interferometry with the Multiple Mirror Telescope and Conventional Telescopes
O. Citterio (Milan)	Infrared Observations with a 12 m baseline Interferometer
C. Froehly (Limoges)	Coherence through Fiber Optics
D. Dravins (Lund)	Search for fine Structure on Stellar Surfaces by Intensity Interferometry

IV. Scientific Importance of High Angular Resolution

1. Planets and Asteroids

T. Encrenaz (Paris)

2. Stars and Star Formation

B. Zuckerman (Maryland)	Circumstellar Envelopes
H.W. Yorke (Göttingen)	Evolution and Appearance of Protostars and their Envelopes
H.J. Habing (Leiden)	Current and Future Observations of Pre-Main-Sequence Objects
P.A. Strittmatter (Tucson)	Preplanetary Disks
A. Blaauw (Leiden)	Binary Stars
E. Schatzman (Nice)	Observations of Stellar Winds and Coronae

3. Extragalactic Objects

G.A. Tammann (Basel)	Normal Galaxies
M.H. Ulrich (ESO)	Nearby Seyfert Galaxies
A. Boksenberg (London)	Radio Galaxies and Quasars: Present and Future Results
M.J. Rees (Cambridge)	Highly Compact Structures in Galaxy Nuclei and Quasars

V. Discussions

Panel discussions will take place on Friday. Topics may include:

- High Resolution in the Space Telescope Era.
- The Future of Interferometry Using Existing Telescopes or Conventional Telescopes under Construction.
- The Scientific Case for Large Interferometers.
- Building Infrared and Optical Interferometers and Budgetary Considerations.

Scientific Organizing Committee: A. Boksenberg, D. Dravins, A. Labeyrie, P. Léna, M.H. Ulrich (Chairman), G. Weigelt.

List of Preprints Published at ESO Scientific Group

December 1980 – February 1981

126. A.C. Danks and M. Dennefeld: Near-infrared Spectroscopy of Comet Bradfield (1979L). *Astronomical Journal.* December 1980.
127. P. Véron, M.P. Véron and E.J. Zuiderwijk: NGC 4507: A Weak Seyfert 1 and X-ray Galaxy. *Astronomy and Astrophysics,* Research Note. December 1980.
128. E.G. Tanzi, G. Chincarini and M. Tarenghi: Infrared Observations of AE Aqr. *Publications of the Astronomical Society of the Pacific.* December 1980.
129. J.H. Oort, H. Arp and H. de Ruiter: Evidence for the Location of Quasars in Superclusters. *Astronomy and Astrophysics.* December 1980.
130. D. Engels, W.A. Sherwood, W. Wamsteker and G.V. Schultz: Infrared Observations of Southern Bright Stars. *Astronomy and Astrophysics Suppl.* December 1980.
131. D. Maccagni and M. Tarenghi: X-ray Observations of Six BL Lacertae Fields. *Astrophysical Journal.* December 1980.
132. W. Wamsteker: Standard Stars and Calibration for JHKLM Photometry. *Astronomy and Astrophysics,* Main Journal. January 1981.
133. J. Danziger, W.M. Goss, P. Murdin, D.H. Clark and A. Boksenberg: The Supernova Remnant in 30 Dor B. *Monthly Notices of the Royal Astronomical Society.* January 1981.
134. G. Chincarini and M.F. Walker: Image Tube Spectroscopic Studies of Rapid Variables. IV. Spectroscopic and Photome-

tric Observations of AE Aquarii. *Astronomy and Astrophysics.* January 1981.

135. Ch. Motch: A Photometric Study of 2A 0526–328. *Astronomy and Astrophysics,* Main Journal. February 1981.
136. M.P. Véron: On the Width and Profile of Nuclear Emission Lines in Galaxies. *Astronomy and Astrophysics,* Main Journal. February 1981.
137. J. Krautter, G. Klare, B. Wolf, W. Wargau, H. Drechsel, J. Rahe and N. Vogt: TT Ari: A New Dwarf Nova. *Astronomy and Astrophysics,* Main Journal. February 1981.
138. N. Vogt: Z. Chamaeleontis: Evidence for an Eccentric Disc during Supermaximum? *Astrophysical Journal.* February 1981.

PERSONNEL MOVEMENTS

STAFF

ARRIVALS

Europe

JANSSON, Jill, S, Secretary, 1.2.1981
BAUDET, Loic, F, Optical Technician, 1.4.1981
BUZZONI, Bernard, Optical Technician, transfer from Chile to Europe, 1.4.1981
BIEREICHEL, Peter, D, Software Engineer, 1.4.1981
COIGNET, Gilbert, F, Electronics Technician, 1.4.1981
DIETL, Ottomar, D, Maintenance Technician, 1.4.1981
STEC, Frédéric, F, Electronics Technician, 1.4.1981
VERSCHUREN, Rita, B, Secretary, 1.4.1981
MÜLLER, Karel, DK, Adm. Assistant (Accounting), 1.5.1981
LJUNG, Bo, S, Electronics Engineer, 16.5.1981
WIRENSTRAND, Hans, S, Systems Programmer, 11.5.1981

Chile

ROUCHER, Jacques, F, Electronics Technician, 1.2.1981

DEPARTURES

Europe

GRIP, Rolf, S, Technical Assistant (Mech.), 31.5.1981
WENSVEEN, Martinus, NL, Optical Technician, 28.2.1981

Chile

BECHMANN, Erling, DK, Foreman (Electro-mech.), 31.3.1981

ASSOCIATES

ARRIVALS

Europe

GAHM, Gösta, S, (part-time) 1.1.1981

DEPARTURES

Europe

CHINCARINI, Guido, I, 15.1.1981

FELLOWS

ARRIVALS

Europe

MOTCH, Christian, F, 1.1.1981
LUND, Glenn, New Zealand, 15.3.1981

The Ionized Gas of M33 as Seen with a 6 m, F/1 Telescope

G. Courtès and J.P. Sivan, Laboratoire d'Astronomie Spatiale, CNRS, Marseille, and J. Boulesteix and H. Petit, Observatoire de Marseille

With few exceptions, the ionized hydrogen regions in a galaxy are extended sources emitting only a few lines of very faint intensity. The use of a narrow interference filter (to select one of the most intense lines) in combination with a focal reducer design (to increase the illumination of the focal plane) at the focus of a large telescope is the best way to obtain deep photographs of the ionized hydrogen features in nearby galaxies (Courtès, G.: 1973, *Vistas in Astronomy* **14,** 81). It should be noted that in this optical arrangement, the filter is not set in the small f-number beam of the focal reducer, but in the lower aperture beam of the telescope, thus making possible the use of very selective interference filters (which accept a very narrow angular field). This method has been extensively used for several years by Courtès and his co-workers at the 1.93 m telescope of Haute-Provence Observatory, at the Palomar 200 inch telescope, and, more recently, at the 3.6 m telescope of ESO.

As previously discussed (Courtès, G.: 1965, IAU Symposium No. 27, A25), when an f/1 focal reducer is attached at the focus of a 2 m class telescope (for instance the f/5 Newtonian focus of the 1.93 m telescope of Haute-Provence), the illumination of the photographic emulsion is increased (by a factor of 25 in this example), but the spatial resolution is unavoidably degraded (a pixel size of 20 microns corresponds to 2.1 seconds of arc). On the contrary, when an f/1 focal reducer is used in combination with a 4 m class telescope or, *a fortiori,* with a larger telescope, the equivalent focal length becomes long enough for the minimum image diameter to be determined mainly by the seeing instead of by the resolving power of the emulsion. In the case of the f/8 Cassegrain focus of the ESO 3.6 m telescope (a project of such an instrument has been designed by M. Leluyer for the 3.6 m ESO telescope), the illumination of the detector is increased by a factor of 64 and the limiting angular resolution is near 1 second of arc for a pixel of 20 microns (Boulesteix, J., Courtès, G., Laval, A., Monnet, G., Petit, H.; 1974, Proceedings of ESO/SRC/CERN Conference on Research Programmes for the New Large Telescopes, 221).

One of the most important results that have been obtained when applying these techniques to the study of the ionized gas of nearby spiral galaxies, is the discovery of a general, diffuse Hα emission in the spiral arms and, sometimes, over the entire galactic disk. (Carranza, G., Courtès, G., Georgelin, Y. P., Monnet, G., Pourcelot, A., Astier, N.: 1968, *Annales d'Astrophysique,* **31,** 63; Monnet, G.: 1971, *Astronomy and Astrophysics,* **12,** 379). In our Galaxy also, the interstellar medium is ionized outside of the condensed, classical H II regions. The presence of a

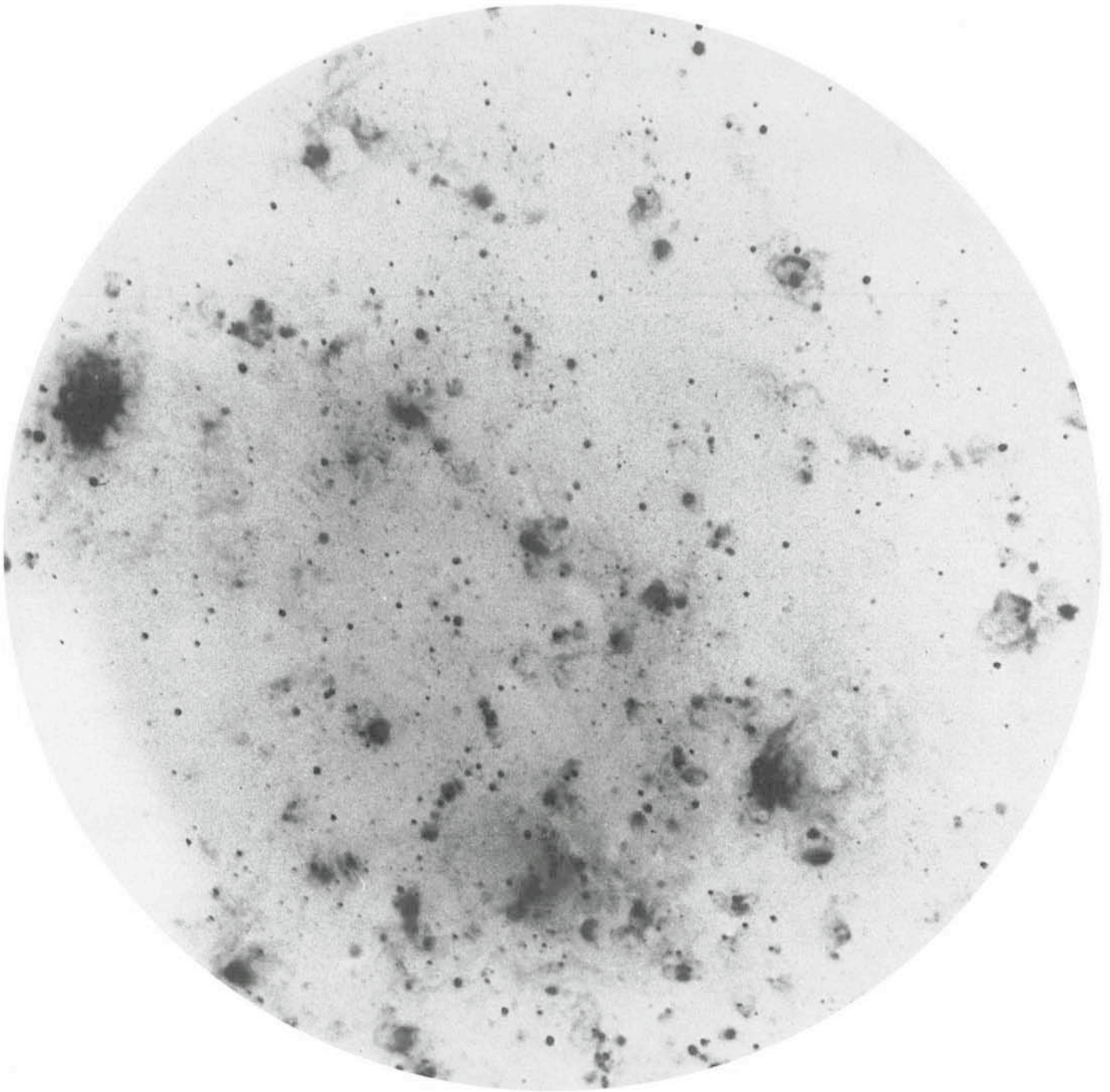

Fig. 1: *Hα photograph of the northern arm of the galaxy M33 taken with the f/ 1 focal reducer of Courtès attached to the prime focus of the Soviet 6 m telescope. This 153 min exposure photograph was obtained in September 1980 on pre-flashed 103-aE film through a 25 Å interference filter peaked at Hα. The field is 20 arcmin in diameter. North is on top.*

general Hα emission background throughout the Milky Way has been revealed by the photographic Hα survey of Sivan (1974, *Astron. Astrophys. Suppl.*, **16,** 163) whose southern part was carried out at La Silla, using a 60° field, interference filter, f/1 camera (Courtès, G., Sivan, J. P., Saïsse, M.: 1981, *Astron. Astrophys.*, in press). These observations are in good agreement with those of Reynolds, R. J., Roesler, F. L. and Scherb, F. (1974, *Astrophysical Journal,* **192,** L53); in addition, they show clearly that the general Hα emission from the arms of the Galaxy is not only diffuse, but faint filamentary structures as well as ring-like and arc-shaped features are seen in between the bright, classical H II regions. The most recent studies of the nearest spirals have not revealed such an appearance for the diffuse ionized gas. This is mainly for reasons of scale.

One of the galaxies best suited for this kind of investigation is the Triangulum galaxy, M33, thanks to its large angular extent (more than one degree) and its favourable inclination (close to face-on). It has been observed in Hα through a 25 Å filter, using the f/1 focal reducer of Courtès at the f/5 focus of the 1.93 m telescope of Haute-Provence (Boulesteix, J., Courtès, G., Laval, A., Monnet, G., Petit, H.: 1974, *Astron. Astrophys.* **37,** 33). A higher angular resolution survey proved necessary in order to investigate small and sharp structures in the Hα emission regions.

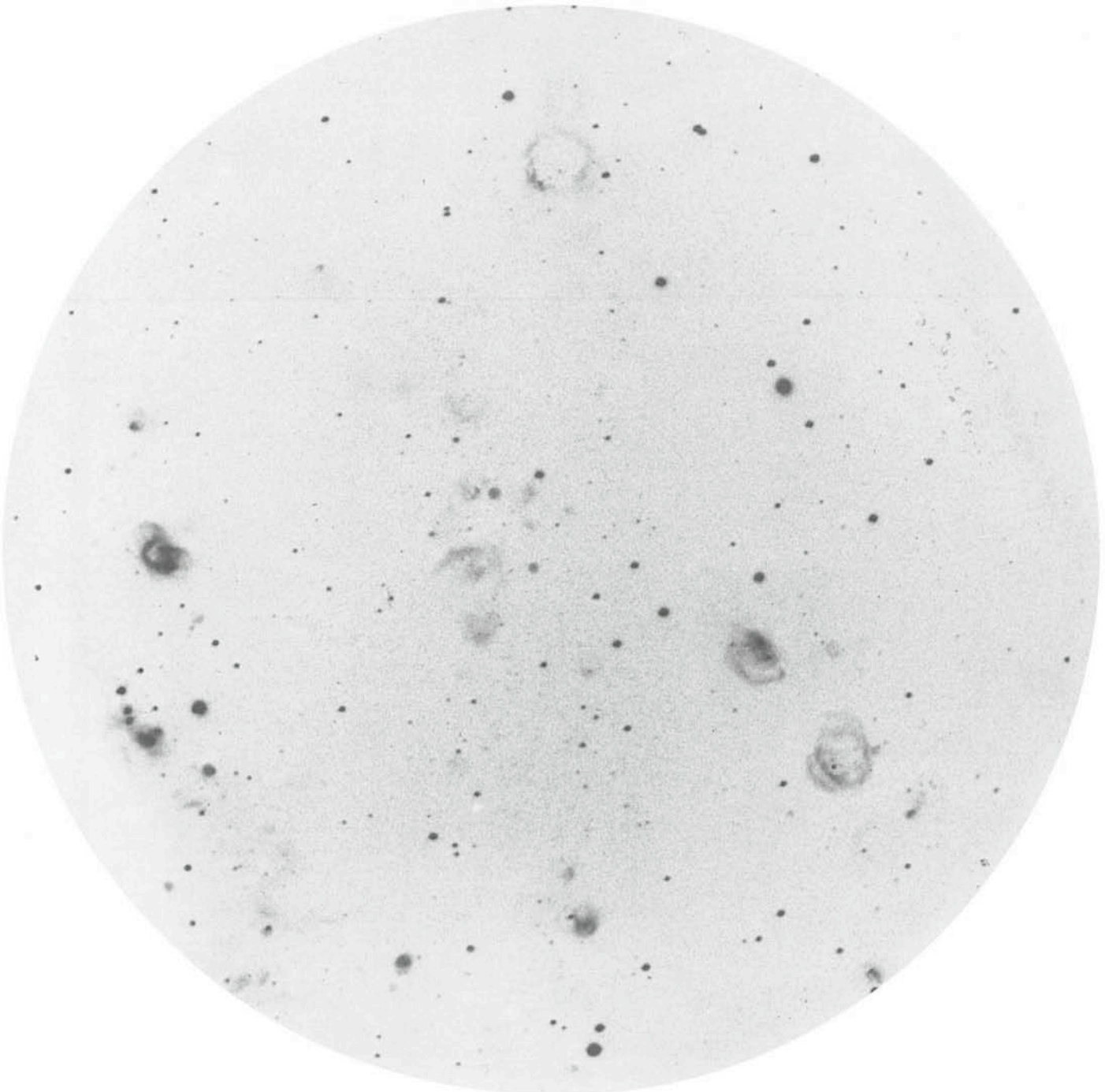

Fig. 2: *Hα photograph of the northern part of the galaxy M33 taken with the f/ 1 focal reducer of Courtès attached to the prime focus of the Soviet 6 m telescope. The centre of the field is 24 arcmin distant from the centre of the galaxy. This 162 min exposure photograph was obtained in September 1980 on pre-flashed 103-aE film through a 25 Å interference filter peaked at Hα. The field diameter is 20 arcmin. North is on top.*

This is the reason why we have adapted (simply by changing the field lens) the f/1 focal reducer to the f/4 prime focus of the 6 m telescope of the Special Astrophysical Observatory. This instrument is the largest optical telescope in the world, located at an altitude of 2100 m in the Caucasus mountain, near Zelentchuk (Soviet Union). The new survey of M33 we have conducted at the 6 m telescope uses the same 25 Å filter to isolate the Hα line and exclude the unwanted continuum from the stars and the atmosphere. The 15 cm diameter of the filter limits a 20 arcmin field, well suited for large-scale studies of extragalactic H II regions.

We show here two juxtaposed fields in the northern part of M33. By comparing these photographs with the ones previously obtained, one notes the fantastic gain on the structures of the H II regions. This is not surprising when one considers that any feature is recorded on the same photographic emulsion on a surface of information 9 times larger. One sees (Fig. 1) the details of this emission: it is far from being uniform and rich in abundant filamentary and arc-shaped structures. On the second photograph (Fig. 2), at the very end of the optical spiral arms, one sees with more details the bubble-like H II regions previously observed with the Haute-Provence 1.93 m telescope. The sharp structure suggests a good similarity with many features of the ionized hydrogen in the Milky Way, like the Barnard and

Cetus Loops and the Gum Nebula (Sivan, J. P., 1974), and with the giant Hα shells observed in the Large Magellanic Cloud (Davies, R., Elliot, K., Meaburn, J.: 1976, *Memoirs of the Royal Astronomical Society,* **81,** 89).

Further investigations (in particular spectroscopic observations) are required to understand the origin of the isolated ring-like structures shown in Fig. 2 as well as that of those observed in the spiral arms (Fig. 1). The energy released in the interstellar medium by supernova explosions and stellar winds may play an important role.

Cyclic Variations of T Tauri Stars

N. Kappelmann and H. Mauder, Astronomisches Institut der Universität Tübingen

During a photographic survey of the Chamaeleon T association in 1971/72, evidence was found by Mauder and Sosna (*Information Bulletin on Variable Stars,* 1049, 1975) for quasi-cyclic light and colour variations of three variable stars, members of this nearby group of young stars. They were classified by Hoffmeister (*Veröff. Sonneberg* **6,** 1, 1963) as T Tauri stars because of their light variations, and this type was confirmed with objective prism spectra by Henize and Mendoza (*Astrophysical Journal,* **180,** 115, 1973).

These three stars, SY Cha, TW Cha and VZ Cha, were observed in the UBV system in the year 1974 by Mauder and twice in the year 1979 by Kappelmann and Mauder, using the ESO standard photometer. Although it could be seen even in 1974 that these three stars show the assumed quasi-cyclic periods, the data of the year 1979 allowed us to confirm these periodic variations and to derive the periods with suitable analysis methods. We derived a period of 7.6 days for SY Cha, 8.6 days for TW Cha and 7.2 days for VZ Cha, and the figures 1, 2 and 3 show the corresponding lightcurves in V.

The colour variations are nearly in phase with the changes in V, and a large ultraviolet excess is found, as expected in T Tauri variables. Thus the photometric measurements not only show variations of the continuum level and the UV excess on time scales of hours or days, a characteristic of the T Tauris, but indicate variations with periods reproducible on time scales of years.

The next step was to confirm these periods with spectroscopic data, but because of the rather faintness of these three systems, with m_V between 12th and 14th magnitude, detailed spectroscopic investigations are difficult. Spectroscopic observations in the blue region were carried out in July 1979 by Mauder, using the Boller and Chivens Cassegrain spectrograph of the ESO 1.5 m telescope. The usable spectral range was about 3600–5100 Å and the spectra were recorded with a dispersion of 58 Å/mm. The observations were carried out on 3 and on 4 consecutive nights, separated by a gap of 12 nights. The spectra are dominated by bright emission lines, among which the strongest lines are H_γ, H_δ, H_8, Ca II K and the Ca II H + Hε blend. The spectra show the typical veiling, a continuous emission in the blue spectral range and exhibit little evidence for an underlying late-type spectrum. As reported by Appenzeller (*Astronomy and Astrophysics,* **71,** 1979), these three stars are members of the YY Orionis type, a subclass defined, among other things, by inverse P Cygni profiles. But we found no evidence for these typical profiles, neither in the Balmer lines, which can be

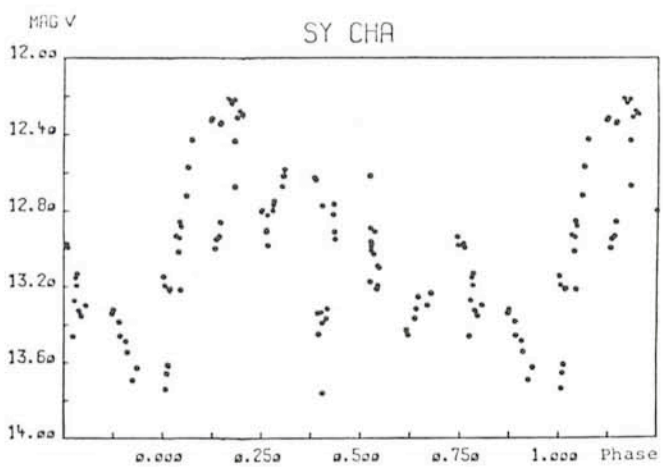

Fig. 1: *Lightcurve of SY Cha, plotted with a period of 7^d.6.*

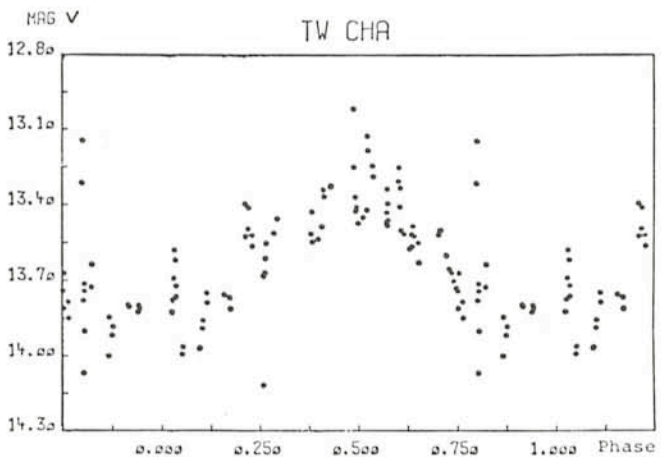

Fig. 2: *Lightcurve of TW Cha, plotted with a period of 8^d.6.*

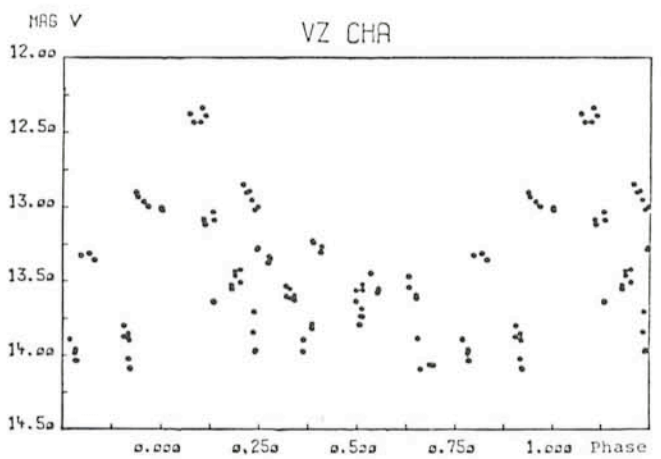

Fig. 3: *Lightcurve of VZ Cha, plotted with a period of 7^d.2.*

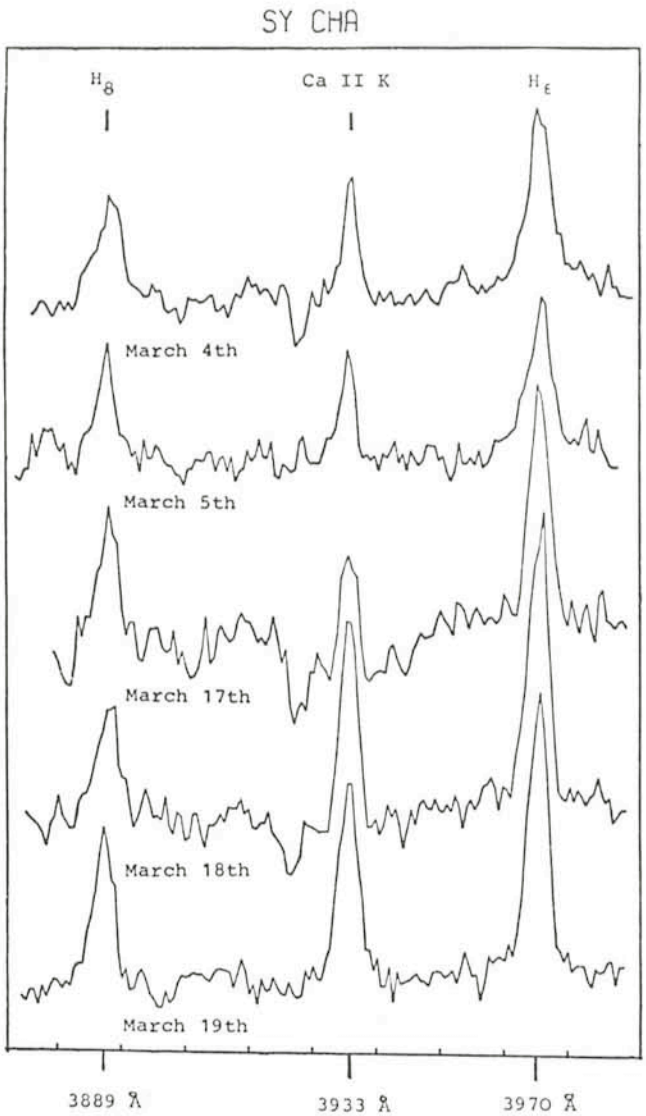

Fig. 4: *Density tracings of the spectrum of SY Cha between the Balmer H_ε and H_8 lines.*

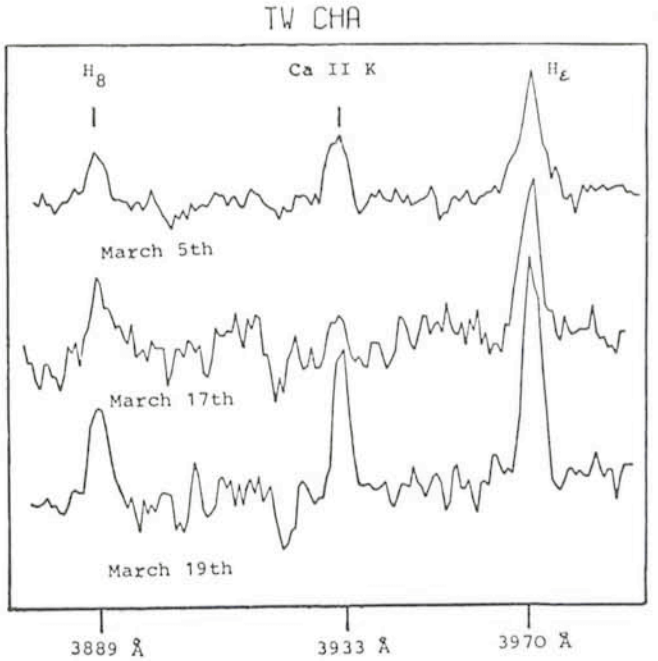

Fig. 5: *Density tracings of the spectrum of TW Cha between the Balmer H_ε and H_8 lines.*

resolved until H_{12} (but the lines with $n > 8$ are rather weak and therefore not very suitable to detect this type of profile, most conspicuous at these lines), nor in the metallic Ca II K line. However, besides a variation of the Balmer lines, there is a complex P Cygni profile of the calcium line, varying strongly within the observational run. In Fig. 4, where the density tracings of SY Cha are plotted, you can see the profile very well in the first spectrum, while vanishing in the second one. Nearly two "photometric" periods later there is again this complex but well seen P Cygni profile in the spectrum of March 17 and it is hardly detected in the last spectrum. A similar behaviour of the Ca II K line of TW Cha can be seen in three selected spectra in Fig. 5.

The lightcurve of TW Cha seems to be well defined, and these three types of spectral features can therefore be attached to the photometric phase of this star. The spectrum of March 5 is correlated to a phase (0.25) of medium luminosity, the spectrum of March 17 is correlated to a phase (0.5–0.6) of high luminosity and the last feature is correlated to a phase (0.9) of low luminosity. This correlation holds true for the other two stars in nearly the same way. Thus we make the conclusion that there is a strong evidence of correlation between the metallic emission line of calcium and its P Cygni profile and the luminosity of the star. But simultaneous photometric and spectroscopic observations based on a time scale of at least two periods are needed to verify this conclusion, to solve the problem of the appearance of different types of P Cygni profiles, and would help to understand the responsible physical processes.

MR 2251–178: A Nearby QSO in a Cluster of Galaxies and Embedded in a Giant H II Envelope

J. Bergeron, Institut d'Astrophysique, Paris

Very extended nebulosities of high excitation have been discovered around a few active galaxies. For the two radio galaxies 3C120 and PKS 2158–380 they extend over dimensions of at least one arcminute (or about 50 kpc) and can be studied in the optical with a reasonable spatial resolution. These observations give information on the interaction between the active nucleus and its surrounding and on the nature of the gaseous envelope.

In the case of 3C120, the luminosity approaches those of QSOs. In addition, a stellar component has been brought into evidence in the brighter parts of the nebulosity.

The strongest lines emitted by these nebulosities are

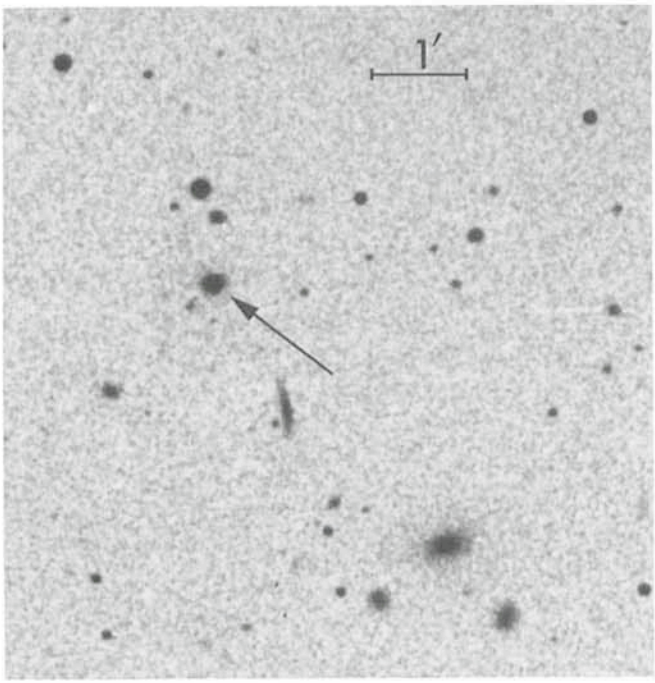

Fig. 1: *The field around the QSO MR 2251–178 from the blue Palomar Sky Survey plate. NE is at the top left corner. The QSO is indicated with an arrow.*

[OIII] λλ 4959, 5007 Å. Spectro-spatial observations of these lines show the motions of the ionized gas. In 3C120 a rotation is discernable, but highly disordered motions are present (Baldwin et al., 1980, *Astrophysical Journal,* **236,** 388). A clear rotation pattern is observed in PKS 2158–30, but the stars do not rotate at all about the rotation axis of the gas (Fosbury, 1980, *The Messenger,* **21,** 11).

The gas observed in 3C120 can simply be the interstellar medium of a normal spiral galaxy and the disordered velocity field could be due to a transfer of momentum from the ionizing radiation escaping the active nucleus. Alternatively the active galaxy may have encountered a gas cloud which is now feeding the nucleus as suggested for PKS 2158–380.

These extended HII nebulosities associated with active nuclei are not a common phenomenon and they are found mainly in radio galaxies. This may reflect some differences in the nuclear activity or differences in the origin and distribution of the gas between Seyfert 1 and radio galaxies.

The hard UV and soft X-ray radiation which escape the nucleus can ionize the gas. This assumption provides a natural explanation for the high excitation of the gas, but is compatible with the observations only if the gas density is low, $n < 1\ cm^{-3}$ (Bergeron, 1976, *Astrophysical Journal,* **210,** 287). The hard radiation spectra in Seyfert 1 and radio galaxies, as derived from EUV and X-ray observations, are very similar and the difference between these two types of galaxies lies probably in the gas distribution.

An observing programme selecting sources with strong UV radiation was started with Alec Boksenberg from University College London, Michel Dennefeld and myself from the Institut d'Astrophysique de Paris and Massimo Tarenghi from ESO. A source of particular interest was the nearby QSO MR 2251–178 discovered from X-ray observations (Ricker et al. 1978, *Nature,* **271,** 35). Its redshift is small, z = 0.064, but the X-ray luminosity is very high, L_X (2 – 11 kev) = 1×10^{45} erg s^{-1}. In the X-ray error circle lies another object, a compact galaxy. The blue Palomar Sky Survey print of the field shown in Fig. 1 reveals the existence of several galaxies a few arcminutes away from the QSO. They constitute an irregular cluster to which the QSO may belong. The QSO is surrounded by a faint nebulosity of 15″ diameter.

Several two-dimensional spectra of the QSO, its surrounding field and a few galaxies of the cluster were taken with the IPCS on the 3.6 m telescope on La Silla. Strong emission lines of high excitation are present in the nebulosity in the close vicinity of the QSO. More striking is the existence of faint [OIII] lines at very large distances (> 100 kpc) from the QSO. Fig. 2 shows these [OIII] lines all the way from the QSO to the south-west galaxy, over a distance of 90″ or 165 kpc (H_0 = 50 km s^{-1} Mpc^{-1}). No nebulosity associated to these lines can be seen in Fig. 1.

This immediately raises the problem of the origin of the gas: is it intracluster gas or is it gas linked to the QSO. The clue to this problem may be given by (1) the overall size of the envelope, (2) its mass, (3) its velocity field.

The HII envelope has an overall size of at least 230 kpc x 60 kpc. Similar dimensions are found for the large HI envelope around the Seyfert 2 galaxy Mark 348 (Morris and Wannier 1980, *Astrophysical Journal,* Letters, **238,** L 7) and for the X-ray emitting gas in groups of galaxies (Schwartz et al 1980, preprint).

From the [OIII] line intensity one can derive an upper limit to the mass of ionized gas. This upper limit is reached if the gas has a homogeneous spatial distribution. The

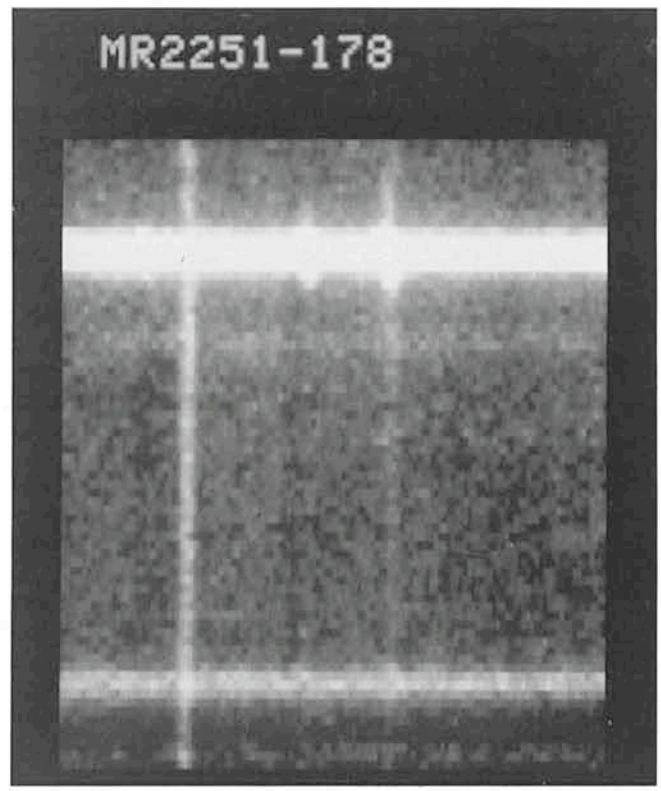

Fig. 2: *A two-dimensional spectrum of the envelope around the QSO MR 2251–178 obtained with the IPCS on the 3.6 m telescope on La Silla. This spectrum shows the redshifted [OIII] lines λλ 4959, 5007Å and the night sky line NI λ 5198 Å. The QSO is at the top and the galaxy SW of the QSO at the bottom. [OIII] λ 5007 runs all the way from the QSO to the SW galaxy.*

mass of ionized gas within a projected area of 230 x 60 kpc^2 is 3 x 10^{10} ($<n>/n$) $M_\odot$ where $<n>$ is the average gas density of the order of 10^{-2} cm^{-3}. If the gas distribution is not homogeneous, the HII mass can be much smaller than 10^{10} $M_\odot$. The range of masses for giant HI halos is $H_{HI} = 10^{10} - 10^{11}$ $M_\odot$, an extreme case being the spiral galaxy NGC 1961 with $M_{HI} = 1.4 \times 10^{11}$ $M_\odot$ (Rubin, Ford and Roberto 1979, *Astrophys. J.*, **230**, 35). The few known X-ray emitting groups (smaller than the well-known large X-ray clusters) have M (hot gas) = $10^{12} - 10^{13}$ $M_\odot$ (Schwartz et al, 1980, preprint). Although the mapping of the nebulosity around MR 2251–178 is incomplete, it seems that the mass of ionized gas falls in the range of masses of HI envelopes around spiral galaxies and this only if the gas is not clumpy.

The kinematics of the ionized gas are derived from the spectro-spatial observations of the [OIII] lines. A clear rotation pattern is detected within 15 kpc of the QSO. In the SW direction, 50 to 150 kpc away from the QSO, the rotation curve flattens. The total spread in velocity in the observed parts of the envelope is 300 km s^{-1}. This is much smaller than the spread in velocity of the galaxies in the nearby groups. The rotation pattern and the continuity in the velocity field over the whole HII envelope strongly favours an association with the QSO.

Stellar absorption lines are seen close to the QSO. The stellar and gas velocities are similar. However, these absorption lines are detected only at a few positions and we cannot derive the stellar velocity field.

It is worth noticing that the few nebulosities studied spectro-spatially up to now have different characteristics and no general scheme can be given. MR 2251–178 is a weak compact radio source and PKS 2158–380 is a strong extended radio source, yet both are surrounded by an ionized envelope in rotation around the nucleus. The weakness of disordered motions in MR 2251–178 contrasts strongly with the highly disordered velocity field around 3C120.

The envelope around MR 2251–178 appears similar to large HI halos around spiral galaxies. The neutral envelope around the Seyfert 2 Mark 348 and the ionized envelope around MR 2251–178 have comparable sizes and masses (if $n \sim <n>$ in the HII envelope) and both show a clear rotation pattern. The difference in their ionization degree may only reflect their different X-ray power. The QSO MR 2251–178 is a very strong X-ray source with $L_x/L_{opt} \simeq 3$, but the Seyfert 2 Mark 348 is a weak X-ray emitter with $L_x/L_{opt} = 1/100$. The envelope around the QSO can easily be powered by the continuum hard energy source and the degree of ionization observed implies $n \lesssim 10^{-1}$ cm^{-2}.

The Dynamics of Elliptical Galaxies

A. Hayli, Observatoire de Lyon, France, and
F. Bertola and M. Capaccioli, Istituto di Astronomia, Padova, Italy

Introduction

Two epochs have to be recognized in the study of elliptical galaxies. Prior to 1975 it was believed that a globally correct description of the structural and dynamical properties of these objects had been achieved. It was thought that these galaxies were well understood, not only because their morphology appeared to be simple and they were considered to contain only *one* stellar population, but also, paradoxically, because of the lack of observational data. Then the observation of the first rotation curve called the validity of the currently admitted ideas in question.

These galaxies look more or less like ellipses whose brightness gradients increase towards the centre. They form a sequence ranging from the circular systems (E0) to the more elongated ones (E6) although a scarcely populated class E7 also exists. The parameter is a measure of the ellipticity of the observed image and may not be immediately related to the spatial shape.

A number of empirical laws, like that of de Vaucouleurs, or semi-empirical, like that of King, have been proposed to describe the brightness distribution of elliptical galaxies. De Vaucouleurs' law gives the surface brightness as a linear function of the fourth root of the distance to the centre. It contains two scale factors and has no free parameter. King's law, devised to describe the observed distribution in globular clusters, is based on the assumption of a quasi-isothermal dynamical model. This law, adapted to elliptical galaxies, makes use of two scale factors. One is the core radius of the galaxy which defines the distance along the bissectrice of the axes at which the projected stellar density, and therefore the brightness, become one half of the values at the centre. The other is the tidal radius, beyond which the brightness is zero. The ratio of these two scale factors is a free parameter in the model.

De Vaucouleurs' law is especially convenient to describe the surface brightness distribution of elliptical galaxies. It is easily compared with observations although it does not perfectly represent the light distribution in the central or peripheral regions of some galaxies like, for instance, M87 or NGC 3379.

Before 1972, the only direct access available to the dynamics of ellipticals was through the observation of the velocity dispersion in the centre which gave an estimate of the random motions of the stars. This quantity, derived by using absorption lines, is difficult to obtain even in the centre. Away from it, the spectrum is barely detectable since the brightness of the galaxy decreases rapidly. Other difficulties are due to the fact that these lines are broad and contaminated by the night sky, sometimes even by interstellar absorption lines. Moreover, the absorption spectrum of a galaxy is a blend of different stellar types and results from the integration along the line of sight. These difficulties explain why no observation of this type was done after the pioneering work of Minkowski (1954, in Carnegie Institution of Washington Year Book **53**, p. 26, 1962, in "Problems of Extragalactic Research", IAU Symp. No. 15, p. 112) and before modern detectors became available. In principle the rotation curve could have been obtained more easily using emission lines. However, not

only very few ellipticals exhibit emission spectra, but also this kind of information does not tell us anything about the dynamics of the stars.

Making use of this rather poor observational background, models were built which gave the illusion that the morphology and dynamical properties of ellipticals were well understood. Simple models were proposed by Prendergast and Tomer (1970, *Astronomical Journal,* **75,** 674) and by Wilson (1975, *Astron, J.,* **80,** 175), following King's quasi-isothermal model. Other, more complex ones have been suggested. They start the description at the collapse phase of the system which ultimately will become a galaxy. Gott's model (e.g. 1975, *Astrophysical Journal,* **201,** 296) described the evolution of a cloud which condenses into stars without dissipation. The hydrodynamical models of Larson (e.g. 1975, *Monthly Notices of the Royal Astronomical Society,* **173,** 671) took into account the dissipation in the gas. In short, we can say that ellipticals were considered to be huge self-gravitating systems of high-velocity stars often flattened because of rotation. Consequently, they were supposed to be oblate spheroids.

We like to emphasize that the observational input to our knowledge of the dynamics of ellipticals was just the measurement of the velocity dispersion in the centres of a few objects. Other observations which now appear to be crucial for the understanding of the spatial configuration of these galaxies existed, by Evans in 1951 (*Mont. Not. Roy. Astron. Soc.,* **111,** 526) and Liller in 1960 and 1966 (*Ap. J.,* **132,** 306; *Ap. J.,* **146,** 28) showing that in some ellipticals the isophotes do not have the same orientation and/or eccentricity. But no attention was paid to these observations until the revision of our ideas on the dynamics of ellipticals took place and further work called new attention to this question. We shall see later how this phenomenon was interpreted in the light of the work, done for instance by Williams and Schwarzschild (1978, *Ap. J.,* **227,** 56) and Bertola and Galletta (1980, *Astronomy and Astrophysics,* **77,** 363).

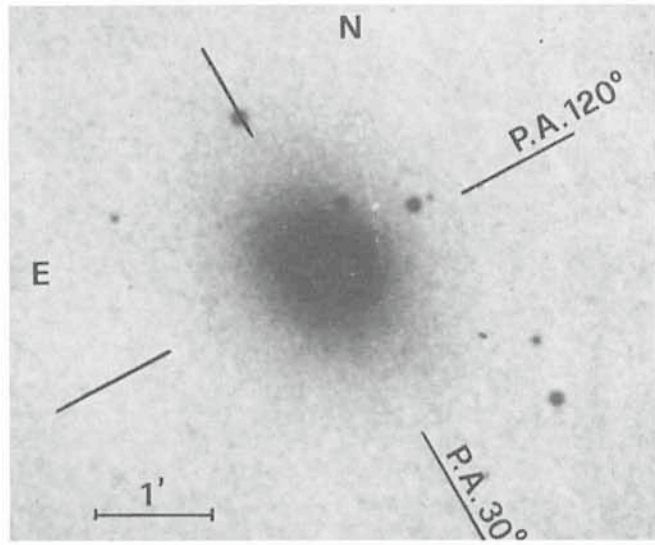

Fig. 1: *The elliptical galaxy NGC 596, reproduced from the Palomar Sky Survey. Despite its very common aspect it displays an unexpected phenomenon: stellar internal velocities along the minor axis, which have recently been confirmed by the authors with the ESO 3.6 m telescope. This result, together with the shape and twisting of the isophotes, suggests a triaxial ellipsoid model. The figure shows the position angles along which the observations have been done. They more or less coincide with the axes of the outer isophotes.*

Recent Observations

The first observations which cast a doubt on the description given above where those made in 1972 by Bertola (Proceedings of the 15th Meeting of the Italian Astronomical Society, p. 199), followed by Bertola and Capaccioli in 1975 (*Ap, J.,* **200,** 439), who published the first rotation curve of an elliptical galaxy, NGC 4697 classified E5. The measurements gave an unexpected result: although this galaxy has an appreciable flattening, its rotational velocity is only 65 km s^{-1}, a very low value indeed. This property has been confirmed for almost all the galaxies so far observed, the maximum velocity being almost always lower than 100 km s^{-1}. Velocity curves along the different axes have been published for about 30 galaxies, and velocity dispersions in the centres, with or without velocity profiles, have been obtained for more than 50 objects. These are basic measurements since kinematical observations are the key to the understanding of the dynamical properties.

Some results have been obtained, due to the improved observing methods, and especially to the use of very sensitive detectors and new reduction techniques. The photon-counting systems allowed to record spectra outside the nuclei of galaxies. The kinematical parameters could be extracted by numerical treatment of these spectra. This is done by correlating the spectrum of the observed galaxy with that of a template star having a spectral type close to that of the galaxy, making use of the Doppler broadening function. For any selected spectral range three quantities are simultaneously extracted at different positions perpendicularly to the dispersion: the redshift and the velocity dispersion and a parameter, usually called γ, which is the mean ratio of the galaxy absorption line strengths to the corresponding ones of the template star.

New observations of this type have recently been made by the authors with the ESO 3.6 m telescope equipped with a Boller and Chivens spectrograph and an IDS (Image Dissector Scanner), which has proved to be satisfactory for this type of work. The four observed galaxies NGC 584, NGC 596, NGC 5128 and A0151–497 represent a sample of normal and peculiar galaxies.

The IDS has two channels for simultaneous observations of the object and the night sky which allow subsequent subtraction. In our observations both slits were used to observe the object. The exposure times were in the range of 30 minutes to two hours. Several spectra were secured during three nights. The subtraction of the night sky was done by using a separate integration.

Except for NGC 5128, the two slits were positioned either symmetrically with respect to the centre, or with one slit at the centre, with different position angles.

The reduction was done in two steps: the transformation of the spectra into absolute flux densities was made in Geneva, using the ESO image processing facilities (now located in Garching). The final analysis, based on the method of Fourier coefficients, using two template stars, was completed in Trieste. Three of the four observed galaxies have some especially interesting characteristics. The fourth one, NGC 584, was chosen because it has a large flattening. The results obtained in this latter case confirm that the rotation is too slow to account for the

flattening. NGC 596 (Fig. 1) was known to show a peculiar phenomenon, radial stellar velocities along the minor axis. Our results confirm this observation which, together with the shape of the isophotes, is one of the best arguments in favour of the triaxial ellipsoid hypothesis.

The two other galaxies are good examples of the class of ellipticals with dust defined by Bertola and Galletta (1976, *Ap. J.* Lett., **226,** L 115). NGC 5128 (Fig. 2) is the prototype and A0151–497 a very good example in the southern sky. The location of the dust in these galaxies suggests that they are prolate spheroids. The observations of the type we have made can contribute to verify the hypotheses. A preliminary result is that in A0151–497 the velocity dispersion tends to show a minimum in the dust lane at a position which corresponds to the centre of the galaxy. A detailed account of these observations will be published by the authors in collaboration with D. Bettoni, G. Galletta, L. Rusconi, and G. Sedmak.

Interpretation

These results have led to discard the classical model in which flattening is due to rotation. It has been suggested for instance that elliptical galaxies are oblate spheroids but with a strong anisotropy of velocities, or prolate spheroids rotating about a minor axis. Fig. 3 from Binney gives the ratio of the maximum rotational velocity to the velocity dispersion at the centre versus the flattening. It clearly shows that the classical model should be discarded and that the new proposed models deserve attention. A third possible model is the slowly rotating triaxial ellipsoid. The assumption that elliptical galaxies are triaxial raises some important problems (see also Binney, 1978, *Comments on Astrophysics,* **8,** 27).

We may assume that elliptical galaxies are self-gravitating stellar systems without collisions. This means that every star moves in the smoothed potential of all the other stars. It may happen that the motions of two stars are perturbed because of a close approach. We say in this case that a close encounter or collision has taken place. However, owing to the relative distances and velocities of the stars in an elliptical, such collisions are rare events and can be neglected on a time scale of the order of the age of the galaxy.

Such a stellar system is described by a distribution function in phase space. This function gives us, for instance, the number of stars which are in a given small region of the configuration space with their velocities belonging to a small given region of the velocities space. If the system is in a steady state, this function does not explicitly depend on time. This assumption is usually made. We know from general dynamics that the motion of any given star in the gravitational field of this kind of galaxy is such that it conserves certain quantities, for instance the total energy, i.e. the sum of the potential and kinetic energy of the star. The total energy is said to be a first integral of the sixth order differential system of equations describing

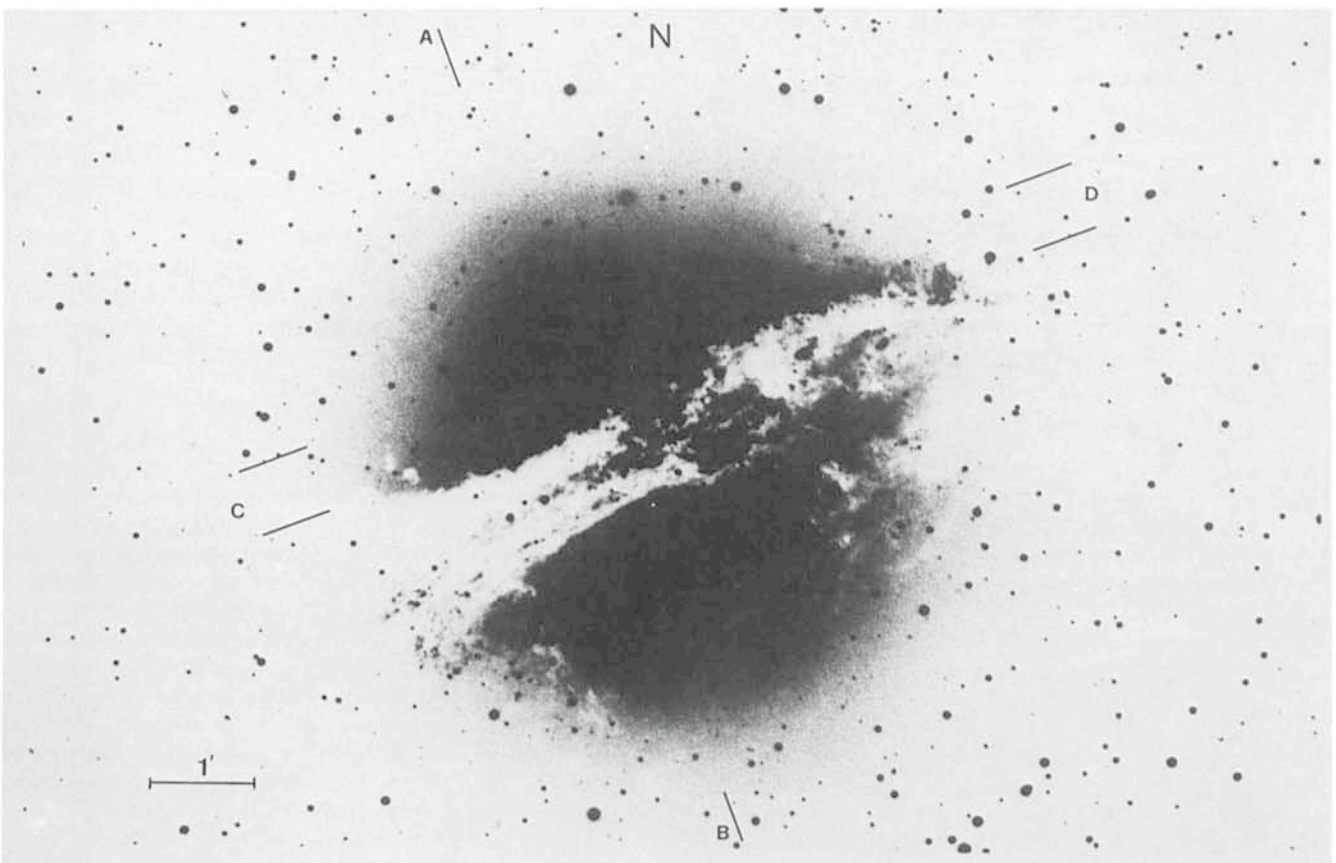

Fig. 2: *The well-known dusty galaxy NGC 5128 has recently been considered as the prototype of a class of galaxies for which the location of the dust suggests that they are prolate spheroids. It has been studied by the authors. The line AB on the photograph (ESO 3.6 m telescope) defines the direction of the two spectrograph slits, the positions of which are shown by the lines C and D. A preliminary inspection of the data indicates that the velocity dispersion near the dust line is about 100 km* s^{-1}.

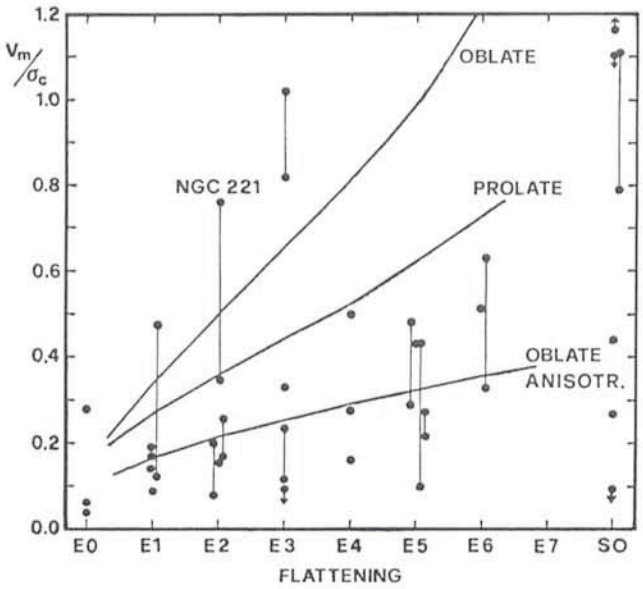

Fig. 3: *On the diagram, the ratio of the maximal observed radial velocity to the central velocity dispersion has been plotted versus the flattening. The curves correspond to different theoretical dynamical models (adapted by M. Capaccioli for* Photometry, Kinematics and Dynamics of Galaxies, *Austin 1979, from Binney 1978). It is seen that observations suggest to discard the isotropic oblate model.*

the motion of the star. More generally, an integral is a function of the variables which becomes a constant when one substitutes in it a solution of the above-mentioned system of equations. One can show that only five independent conservative integrals exist.

A theorem of Poincarė (but often referred to as Jeans theorem) says that the distribution function which is a solution of Liouville partial derivative equation, is an arbitrary function of conservative and isolating integrals of the equations of motion of a star. The mathematical definitions of isolating and non-isolating integrals are rather complicated (see for instance Contopoulos 1963, *Ap. J.*, **138,** 1298). We shall give here a simple geometrical representation of these integrals without any aim of being rigorous.

Phase space has 6 dimensions: 3 for space coordinates and 3 for velocity coordinates. Let I be a first integral. Then the equation $I = C$, where c is a constant, defines a region in phase space. I is said to be isolating in this region if the equation $I = c$ can be solved with respect to all the variables, giving a finite number of solutions. $I = c$ is then a "good" hypersurface. Classical integrals are of this kind. Non-isolating integrals are of two types: *ergodic* and *quasi-isolating*. An integral I is said to be ergodic if in the neighbourhood of any point in the above-mentioned region one can find some points where it can take values which are as different as we can think. It can also be said that the hypersurface $I = c$ goes as near as we want from any point in the region. The corresponding orbit in the 3-dimension configuration space is also called ergodic. An isolating integral brings restrictions to the motion in phase space and to the motion of the star in the 3-dimensional space as well. An ergodic integral does not so. An integral is said to be quasi-isolating if it is non-isolating in the above-defined region, but does not go through the neighbourhood of *all* its points. In fact the properties of quasi-isolating integrals make them similar to isolating ones. They can be arguments of the distribution function. Simple examples can be given of non-isolating integrals in well-known potentials, for instance the two-dimensional harmonic oscillator. Let us also mention that integrals can be stable, quasi-stable or unstable with respect to some type of perturbation of the potential.

The equations of motion of a star which moves in the field of a spheroid have two classical isolating integrals: energy and the projection of the star's angular momentum on the axis of symmetry. In general no other integral is known which can be given analytically. However, numerical investigation has shown that for some stars a third isolating integral exists. Sometimes the third integral is only quasi-isolating. It is well known for instance that the local distribution of velocities in the Galaxy is not, as one would expect, symmetrical with respect to the direction of the Sun's motion. It is thought that this effect is due to the existence of a third integral for some of the stars. (As the Galaxy is axisymmetric, the motion of a star has the classical two integrals. The last two integrals are non-isolating.)

In a similar way, it may be that the dynamics of elliptical galaxies depend on the distribution of the values of a third integral among the stars. In this case, flattened axisymmetric systems with a slow rotation but a strong velocity anisotropy could exist.

Let us assume now that for some stars of an elliptical galaxy two non-classical isolating integrals exist. This galaxy could then be triaxial. In this case, there is only one classical integral, namely the energy. We may then imagine that one of the non-classical isolating integrals would control the amplitude of the star's oscillations along the main axis. However, Vandervoort (*Ap. J.*, 1980, **240,** 478) has recently shown that triaxial systems in equilibrium may exist without any isolating integral except that of Jacobi, and he has drawn attention to the fact that Jeans theorem does not require that the distribution function should be a function of *all* the isolating integrals. But the models illustrating these results are not realistic for representing elliptical galaxies.

The work of Aarseth and Binney (1978, *Mont. Not. Roy. Astr. Soc.*, **185,** 227) and of Schwarzschild (1979, *Ap. J.*, **232,** 236) shows that satisfactory triaxial configurations seem possible and that they could last. The study of orbits in the field of a triaxial homogeneous ellipsoid shows that most of them are not ergodic and that there are two non-classical isolating integrals (Contopoulos 1963, *Astron. J.*, **68,** 1). The work of Schwarzschild suggests that self-coherent triaxial systems in dynamical equilibrium, which have density profiles like those of elliptical galaxies, may exist. Aarseth and Binney's work brings encouraging results on the fate of triaxial initial configurations which seem to keep their shape after the violent relaxation which could have proceeded the equilibrium state. On the other hand, Contopoulos (*Zf. f. Astrophys.*, 1956, **39,** 126) has shown that observations do not exclude the existence of triaxial structures: the observed shapes of the isophotes of elliptical galaxies could be the projection of spheroids as well as of triaxial ellipsoids. Finally *N-body* numerical experiments by Miller (1978, *Ap. J.*, **223,** 122) have produced such triaxial configurations.

Let us now recall the results on the twisting of the isophotes, which were described at the end of the introduction. This characteristic, shown by NGC 596, can be given two interpretations: either the galaxy has isodensity surfaces which are spheroids with axes of different

orientations; or, more probably, these surfaces are triaxial ellipsoids which have the same orientation, but whose axes have different ratios. The twisting of the isophotes could then be considered as a projection effect. We see therefore that photometric studies bring a strong argument in favour of the triaxial ellipsoid hypothesis and that there are non-classical isolating integrals that may help elliptical galaxies to keep their shapes.

So there is no reason to suppose that elliptical galaxies are necessarily spheroids since the most general configurations are triaxial. As long as it was not realized that non-classical integrals exist that could shape lasting triaxial configurations, it was natural to believe that elliptical galaxies were spheroids. This is because an initial triaxial distribution could not be preserved after the dynamical mixing phase which lasts for less than 10^9 years. Now recent works seem to show that in order to produce a spheroidal rather than a triaxial galaxy one must start with peculiar initial conditions, that is from a configuration in which the isodensity surfaces have their same two main axes equal.

Let us mention a very recent work to be published by Miller and Smith. These authors suggest on the basis of numerical experiments that most elliptical galaxies have reached their present state in two steps. They may have taken first the shape of a bar (prolate spheroid) during a protogalactic collapse controlled by rotation. Then they would have been slowed down by tidal interaction with their neighbourhood to finally rotate as slowly as shown by observations.

Conclusion

The revolution in the field of elliptical galaxies is going on. But we are far from knowing for sure what are the actual shapes and the dynamics of these objects. Many questions remain unanswered. For instance:

If ellipticals are triaxial now, will they keep their shapes for a long time? We do not know how to write non-classical integrals and we are not sure whether they are isolating or non-isolating, stable, quasi-stable or unstable.

Are triaxial galaxies generally closer to oblate or to prolate spheroids? How are galaxies distributed among these varieties? What is the rotation of these systems as a whole?

Elliptical galaxies give rise not only to dynamical problems. We also would like to know about nuclei, interactions with the neighbourhood and resulting evolution, evolution of the stellar content, etc.

The least we can say is that, contrary to the idea which was prevailing not so long ago, elliptical galaxies are very complex systems.

The Pre-Main-Sequence Shell Star HR 5999 Unveiled

P.S. Thé and H.R.E. Tjin A Djie, Astronomical Institute, University of Amsterdam

The star HR 5999 is embedded in a dusty gaseous nebulosity and is surrounded by more than 10 faint T Tauri stars. From these facts and from studies so far made of the physical properties of HR 5999, we strongly believe that it is a very young pre-main-sequence object; it varies irregularly due most probably to changes in the properties of dust grains embedded in its circumstellar gas shell.

In 1978 a campaign of simultaneous observations of the variable pre-main-sequence shell star HR 5999 from several observatories in the world was organized. At approximately maximum brightness ($V = 7\overset{m}{.}0$) the star was observed in the ultraviolet with the IUE, in the visual with Walraven, Johnson and Strömgren photometers, in the red and the near infrared with photometers attached to the ESO 1 m telescope. Near infrared and visual measures were obtained at the South African Astronomical Observatory. Furthermore, polarimetric and spectroscopic observations were also made. A description of this international campaign was given in *Messenger* No. 16 (March 1979). In this article the first results of the study of the photometric data and preliminary notes on the spectroscopic material are described.

Interstellar and Circumstellar Extinction

HR 5999 (= V 856 Sco) is one of the brightest pre-main-sequence stars. We have been studying this star for several years now. Due to particularly favourable circumstances it is possible to penetrate deeply into the extended atmosphere of this irregular variable star. Before its light arrives on earth it has to go through circumstellar material and through foreground interstellar medium. The way this light is attenuated by the latter is well known, but the manner in which it is dimmed by circumstellar dust grains is often different. This, in general, entails the problem of separating both types of extinction. In the case of HR 5999 it is possible to estimate the amount of foreground extinction, because it has a common proper motion companion, HR 6000, separated at an angular distance of only 45". The amount of foreground extinction suffered by the light of the companion is about the same as that by the light of HR 5999. Being located at a distance of approximately 270 pc only, the amounts of foreground colour excess and extinction are, actually, not excessively large: $E(B-V) = 0\overset{m}{.}06$ and $A_V = 0\overset{m}{.}19$.

The star HR 5999 varies in the visual often about 1 magnitude in brightness, simultaneously with its change in colour index, in the sense that the star becomes redder when its light weakens. In general, the determination of the extinction by circumstellar matter is difficult. In the case of HR 5999 there are, however, strong indications that it is this material which causes the star to vary in brightness irregularly, perhaps triggered by a phenomenon which occurs closer to the surface of the star. Additional evidence for such a phenomenon is provided by the observations of linear polarization made simultaneously with the photometric measurements. They indicate that the degree of polarization is varying in phase with the change in colour index.

Based on the way the variations in brightness and the simultaneous changes in colour index are correlated, it is possible to derive the character of the extinction law of the circumstellar dust grains. A value for the ratio of total to selective extinction, $R = A_V/E(B-V)$, anomalously larger than for the normal interstellar dust grains was found: $R = 4.37$. Having also E(B-V) for the circumstellar matter separately, it is then not difficult to calculate A_V and A_B for this material: $A_V = 0.17$ and $A_B = 0.21$ at maximum brightness.

The Energy Distribution

Using the foreground interstellar colour excess discussed above it is possible to determine the interstellar extinction at the different passbands based on the normal extinction law.

The spectral energy distribution of HR 5999 at about its maximum brightness V = 7 m0, is depicted in Fig. 1 by the thick line. The ultraviolet part of this energy distribution was derived from low resolution IUE spectral observations, folded at the five ANS passbands. It should be noted that in order to obtain the true spectral energy distribution of HR 5999, the circumstellar extinction must be taken into account. Two points of the true spectral energy distribution are known at the effective wavelengths of the B and V passbands, using A_B and A_V obtained above. These points are indicated by black squares in Fig. 1.

From spectrograms we know that HR 5999 is of spectral type A7 III. In the literature we have found two bright unreddened stars of the same spectral type (θ Tau and HR 3270) which were observed by Johnson in the visual, red and near infrared, and by the ANS in the ultraviolet. From the mean value of these observations we have derived an extinction-free spectral energy distribution, which is also shown (thin line) in Fig. 1, normalized at the two extinction-free points (black squares) of HR 5999. For comparison purposes we also show, by circles, the spectral energy distribution derived by Kurucz for a star of $T_{eff} = 7750$ K and log g = 3.0. The agreement is quite good. We now assume that the true spectral energy distribution of HR 5999 is not much different from the above-mentioned one.

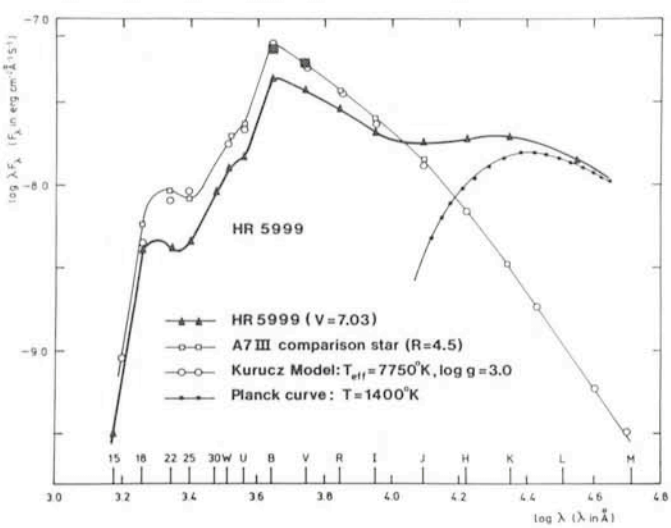

Fig. 1: *The spectral energy distribution of the star HR 5999 (thick line) freed from foreground interstellar extinction, compared to that of a Kurucz Model and of an unreddened mean A7 III comparison star. (Reproduced from* Astronomy and Astrophysics Supplement Series.)

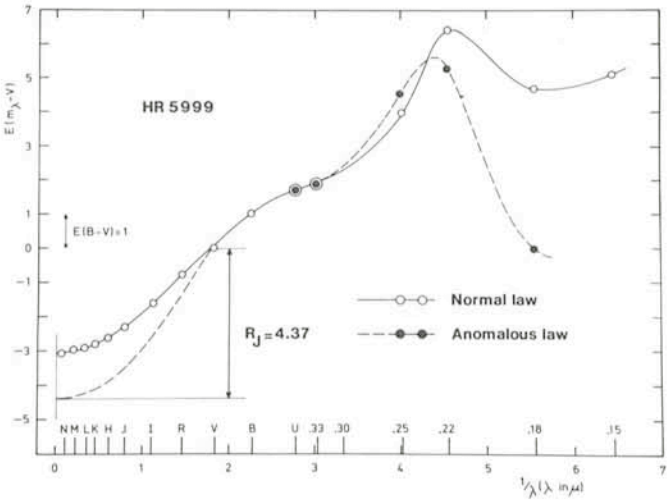

Fig. 2: *The extinction law of the circumstellar material of the star HR 5999. In the infrared as well as in the ultraviolet this law is anomalous. (Reproduced from* Astronomy and Astrophysics Supplement Series.)

The Energy Balance

Fig. 1 shows that the ultraviolet, visual and red energy emitted by the star HR 5999 is absorbed by the dust particles in the circumstellar shell. The total energy lost by the star to these dust grains, as estimated on earth, is about 1.5×10^{-8} erg cm^{-2} s^{-1}. This is about 25% of the total intrinsic energy of HR 5999.

From Fig. 1 it is also clear that the absorbed energy by the dust grains is re-emitted in the infrared spectral region. This re-emitted energy can also be estimated. Up to 5 μm it turns out to be about 1.7×10^{-8} erg cm^{-2} s^{-1}. More towards the infrared the amount of re-emitted energy becomes negligibly small. Considering the errors in their determinations, it can be concluded that the absorbed energy (UV, visual and red) is in good balance with the re-emitted energy in the infrared.

It is of interest to know the temperature of the absorbing dust grains. If we assume that the thermal dust radiation can be approximated by a Planck distribution, it is possible to fit the distribution of the excess infrared radiation at the long wavelength slope with a Planck curve. The temperature of the dust grains characterized by this curve is about 1400 K.

Other physical characteristics of the dust grains can be derived. If it is assumed that our previous determination of grain size, 0.16 μm, is not far from the truth and if it is further assumed that the grains are composed of C or Fe, then it can be calculated that the radiating grains are located about 1.8 AU from the surface of the central star. However, if the dust grains are composed of Si_2O_3 or Si C, then they are lying more than 3 times further away: 5.8 AU. The corresponding total dust shell masses are 4×10^{-11} and 9.5×10^{-10} $M_\odot$, respectively.

The Circumstellar Extinction Law

It has been shown that the circumstellar extinction law is anomalous. The value of the ratio of total to selective extinction is larger than normal: $R_J = 4.37$. This extinction law is depicted in Fig. 2. The question is then: How is the behaviour of the circumstellar law in the ultraviolet? To answer this question, the extinction-free and real ultraviolet energy distribution have been compared, so that the UV circumstellar extinction law of the star HR 5999 could be

Fig. 3: *The shell star HR 5999 unveiled. An artist's impression. Courtesy Mrs. M. Moesman.*

derived. It is shown in Fig. 2 as an extension of the visual part of the law. Compared to the normal extinction law of interstellar matter, the behaviour of the UV circumstellar law is completely different. The 2200 Å bump is somewhat lower and shifted towards larger wavelengths Furthermore, at about 1800 Å it is very much lower, resembling that for the star σ Sco reported by Savage.

The Spectrum

A study was made of the red and blue spectral plates (12 Å/mm) of HR 5999 taken in May 1978. Many lines of H I, Ca I, Fe II and Ti II are present and are composed of a broad photospheric component and several blue-shifted shell components. There are, however, lines which are purely photospheric (e.g. Mg II λ 4481) whereas other lines have only shell components (Na I D). The H-alpha line is in emission and has variable double structure. This variation appears to be in antiphase with the brightness changes of the star. Low resolution IUE spectra, taken also in May 1978, show in the short wavelength range ($\lambda < 2000$ Å) the presence of emission lines of O I, C II, C IV and probably Al II; in the long wavelength range (2000 Å $< \lambda <$ 3000 Å) there are indications of strong and broad absorption features. A steep drop-off of the continuum at about 1800 Å is in agreement with the spectral type A7 derived earlier from the red and blue plates. High resolution IUE spectra of the long wavelength region, taken more recently by Hack and Selvelli, reveal the presence of many shell lines from multiplets of Fe II, Cr II and Mn II in absorption and strong emission of the Mg II λ 2800 doublet with a double structure, comparable with that of H-alpha.

The radial velocities of the shell components on the blue and red plates vary in time between –40 and –5 km/s, more or less in phase with the variation of the dust extinction. Because of the large width of photospheric lines their radial velocites are more difficult to determine. The values vary between –20 and +20 km/s.

Although many details of the spectra are still being studied, the spectral data support our believe in the existence of a hot emission shell (C IV emission line) around the star, surrounded by a cooler, less dense shell region, where the shell absorption components are formed and in which the circumstellar dust is embedded. If this is true, one can imagine that the dust extinction and polarization variations are the result of changes in the character of the dust grains due to perturbations in the photosperic or hot shell region, which are propagated outward supersonically through the cooler dusty surroundings. The cause and the characteristics of the perturbations are not yet clear, but the existence of instabilities in the shell of HR 5999 can be expected in view of the evolutionary stage of this pre-main-sequence star.

A Supernova Discovered at La Silla

Dr. André B. Muller from ESO recently described (*The Messenger* No. 19, p. 29, 1979) a new system allowing an easy and efficient monitoring of galaxies for the detection of supernovae. Using this system, H.E. Schuster discovered a supernova in NGC 1255 on December 30, 1980 (*IAU Circular* No. 3559, 1981). At the time of discovery its magnitude was 17. This was the first supernova found on La Silla.

Thanks to the kind collaboration of Visiting Astronomers Dr. W. Seitter and Dr. H. Duerbeck, an immediate follow-up was carried out, showing that it was a type II supernova.

P. V.

ESO/ESA Workshop on "Optical Jets in Galaxies"

With the aim of encouraging European cooperation and coordination in the use of the Space Telescope within some fields of research, ESO and ESA have arranged a series of workshops on the use of the Space Telescope and coordinated ground-based observations. The second of these workshops, entitled "Optical Jets in Galaxies", took place in the auditorium of the new ESO Headquarters in Garching on February 18–19, 1981.

Thanks to active contributions from 50 participants from different institutions in Europe and the USA, the meeting was very successful. Optical, radio and ultraviolet observations of jets were discussed in great detail. One of the results of the meeting is that the Space Telescope is expected to play a key role in the study of jets because of high resolution and UV sensitivity. The workshop proceedings will be published in a short time by the ESA Press.

M. T.

ALGUNOS RESUMENES

Observaciones "Speckle" en infrarrojo realizadas con una cámara de televisión

En principio, los grandes telescopios, como el de 3.6 m de la ESO, tienen una resolución angular mejor que 0.1 segundo de arco, vale decir, que detalles asi de pequeños pueden ser vistos; pero comúnmente éste no es el caso. Las mejores fotografias tomadas con grandes telescopios pocas veces muestran detalles más pequeños que 1 segundo de arco (un segundo de arco es la separación angular de dos puntos separados por un milimetro a una distancia de 200 metros); ésto se debe a la presencia de la atmósfera que es turbulenta, y esta turbulencia produce una imágen borrosa del objeto.

The ESO MESSENGER is published four times a year: in March, June, September and December. It is distributed free to ESO personnel and others interested in astronomy.
The text of any article may be reprinted if credit is given to ESO. Copies of most illustrations are available to editors without charge.

Editor: Philippe Véron
Technical editor: Kurt Kjär

EUROPEAN
SOUTHERN OBSERVATORY
Karl-Schwarzschild-Str. 2
D-8046 Garching b. München
Fed. Rep. of Germany
Tel. (089) 320 06-0
Telex 05-28 282-0 es d

Printed by Universitätsdruckerei
Dr. C. Wolf & Sohn
Heidemannstraße 166
8000 München 45
Fed. Rep. of Germany

Los astrónomos denominan ésto "seeing"; y ellos se sienten bastante contentos cuando el "seeing" se reduce a un segundo de arco. Hace aproximadamente 10 años, un astrónomo francés, Dr. Antoine Labeyrie, notó que exposiciones de extremadamente corta duración (de sólo algunas centésimas de segundos) de estrellas brillantes muestran detalles (llamados "speckles") que son tan pequeños como la resolución teórica del telescopio, y desarrolló una técnica (interferometria speckle) que permite extraer la información que contiene un gran número de fotografias de corta exposición de un sólo objeto.

En el campo óptico esta técnica es usada hoy en dia por un gran número de grupos en todo el mundo. Recientemente los Drs. P. Lamy y S. Koutchmy han realizado con éxito varios tests en La Silla que mostraron que esta técnica también puede ser aplicada en el infrarrojo (a 1.6 μm).

El gas ionizado de M33 visto con un telescopio de 6 m

Generalmente las regiones de hidrógeno ionizado (H II) en una galaxia son fuentes que emiten sólo algunas lineas de muy baja intensidad. La mejor manera para obtener fotografias detalladas de las estructuras de hidrógeno ionizado en galaxias cercanas es usar un filtro de interferencia angosto para seleccionar una de las lineas más intensas, en combinación con un reductor focal para aumentar la iluminación del plano focal en el foco de un gran telescopio.

Debido a su gran extensión angular y a su favorable inclinación, M33 es una de las galaxias más apropiadas para investigar las estructuras de H II.

Cuando fue observada por primera vez por el Dr. Courtès y sus colaboradores con el telescopio de 1.93 m de Haute-Provence, usando un filtro de interferencia angosto y un reductor focal, se hizo evidente que se requeria una mayor resolución angular para poder obtener más detalles de las estructuras de hidrógeno ionizado. Ya que la resolución angular aumenta con el tamaño del telescopio, el reductor focal del Dr. Courtès fue adaptado al foco primario del telescopio de 6 m en la montaña del Cáucaso, cerca de Zelentchuk en la Unión Soviética.

En las páginas 16 y 17 se pueden apreciar dos fotografias tomadas con este instrumento, que es el telescopio óptico más grande en el mundo. Ellas muestran más detalles que cualquier otra fotografia tomada antes de la misma región y más estudios serán necesarios para entender el origen de las varias estructuras que se pueden apreciar en las placas.

Contents